Evaluated Theoretical Cross Section Data for Charge Exchange of Multiply Charged Ions with Atoms. I. Hydrogen Atom-Fully Stripped Ion Systems

R. K. Janev,[a] B. H. Bransden,[b] and J. W. Gallagher

Joint Institute for Laboratory Astrophysics, University of Colorado and National Bureau of Standards, Boulder, Colorado 80309

The existing theoretical cross section data for the charge exchange process of multiply charged fully stripped ions with hydrogen atoms are evaluated in the energy range from ~ 10 eV/u to $\sim 10^3$ keV/u. The evaluation has been performed on the basis of both pure theoretical arguments and comparison with the most accurate experimental cross sections. The ionic charge state ranges from $Z = 2$ to $Z = 54$. The theoretical methods for calculation of the charge exchange cross sections are briefly discussed, and their regions of validity and the accuracy of the produced data are assessed.

Key words: charge exchange; cross sections; hydrogen atom; fully stripped ions; multiply charged ions.

Contents

1. Introduction

The collision processes of multiply charged ions with atoms play an important part in many high temperature laboratory and astrophysical plasmas. Among them, the charge exchange process is of special importance, because for a wide range of collision energies it is a dominant process (with the highest cross section) and because it leads to the creation of excited (radiating) reaction products. The charge exchange cross sections of multiply charged ions are needed for modeling and diagnostics of high temperature plasmas, in particular of the tokamak type of fusion plasmas, where multiply charged ions are present as impurities.

In view of the important practical implications of the charge exchange of multiply charged ions with atoms, extensive investigations of this process, both experimental and theoretical, have been carried out in the past decade. The results of these investigations have been presented in several review articles.[1-4] Theoretical studies of this process have led to important developments of the underlying collision dynamics and to the accumulation of a significant amount of cross section data. A critical analysis of these data, as well as of the methods used for their production, is now a necessary step, which will be helpful in the practical use of the data and the methods.

The present paper attempts to provide such an analysis of the theoretical methods and cross section data for charge exchange reactions between hydrogen atoms and completely stripped ions.

$$\mathrm{H}(1s) + \mathrm{A}^{Z+} \rightarrow \mathrm{H}^{+} + \mathrm{A}^{(Z-1)+}(n\ell m), \qquad (1)$$

where n, ℓ, m are the usual quantum numbers of the captured electron and Z is the ionic charge. Our objectives are the following: (1) to assess the intrinsic strengths and limitations of various theoretical methods currently used for charge exchange cross section calculations with multiply charged ions and thereby define the regions of their validity with respect to the collision velocity and ionic charge, (2) on the basis of these assessments and by comparison with experimental data (when such data exist), to evaluate the existing theoretical cross section data, and (3) to present the most accurate data in a form useful for practical applications. The energies in this paper are quoted in the form of the laboratory energy of the ion (E) in eV (or keV or MeV) divided by the mass of the ion (M) expressed in atomic mass units (u). The energy range covered is from ~ 10 eV/u to ~ 1 MeV/u, in which almost all of the calculations have been done and which is the chief region of practical importance.

In two forthcoming papers, we shall present evaluated theoretical cross section data for the reaction of hydrogen atoms with incompletely stripped ions and for atoms other than hydrogen with arbitrarily stripped ions.

The importance of an evaluated compilation of the theoretical charge exchange cross section data stems from

[a] JILA Visiting Fellow, 1981–82. Permanent address: Institute of Physics, Belgrade, Yugoslavia.

[b] JILA Visiting Fellow, 1981–82. Permanent address: Department of Physics, University of Durham, Durham, England.

the lack of experimental data for many atomic and/or ionic species. Even when such data exist they usually cover a rather restricted energy range.

2. Theoretical Methods for Charge Exchange: Validity Regions and Accuracies

The collision dynamics of a charge exchange process depend on the relative velocity of the colliding particles v and the ionic charge Z. With respect to the parameter v, it is useful to distinguish three broad regions: $v \lesssim v_0$ ($v_0 = e^2/\hbar = 2.19 \cdot 10^8$ cm/s is the velocity of the electron in the ground state hydrogen atom), $v \gtrsim v_0$, and $v \gg v_0$. In each of these velocity regions, different groups of theoretical methods have been developed to describe the charge exchange process. Below, we shall analyze these methods briefly from the point of view of their regions of validity with emphasis on the accuracy they can provide in the cross section calculations. The laboratory collision energy per nucleon is related to the collision velocity v by $E/M = 25(v/v_0)^2$ (keV/u).

2.1. Low-Energy Methods

In the low-velocity region $v \lesssim v_0$, the charge exchange process is best described within the framework of a quasimolecular picture. The collision dynamics are described by a set of close-coupled equations obtained from an expansion of the scattering wave function in terms of molecular orbitals of the colliding system. This method is generally referred to as CC-MO (close-coupling of molecular orbitals). In certain extreme physical situations, the CC-MO method can be reduced by the use of simplifying models. Three different approaches have so far been developed and used for charge exchange cross section calculations in this velocity region: the perturbed stationary state (PSS) method,[5] the multichannel Landau–Zener model (M-LZ)[6] and different decay models (DM).[7–9]

a. The PSS Method

The scattering equations in this method are obtained from an expansion of the total wave function in terms of the adiabatic molecular orbitals of the colliding system. The use of this expansion basis leads to Galilean noninvariance of the coupled equations, difficulties in satisfying the boundary conditions for the problem, nonzero coupling matrix elements for the dipole transitions in the separated-atom limit, and dependence of the results on the choice of the coordinate system in which the matrix elements are calculated (see, e.g., Ref. 10). In order to overcome these difficulties, suitable translational phase factors must be associated with the basis functions, designed in such a way as to describe the electron momentum transfer and to satisfy the asymptotic conditions. Although many attempts have been made in this respect,[11–13] no satisfactory solution of the problem has yet been reached. The procedure of the variational optimization of the translational factors seems to be the most promising.[10,13] However, inclusion of sophisticated translational factors in the basis functions leads to significant difficulties in numerical computations. Reduction of these difficulties by a simplified treatment of the problem of translational invariance reduces the accuracy of the results obtained. The accuracy of the PSS method also depends on the number of states included in the basis set. A study of the very many PSS cross section calculations (see Sec. 4) performed with straight line trajectories for the nuclear motion lead to the following conclusions:

(1) If no translational factors are included, the uncertainty of the computed total cross sections may be of order of 100% at $v \approx 1v_0$, 20% at $v \simeq 0.2v_0$, and less than 10% for $v \lesssim 0.1v_0$, where it is assumed the number of basis states is $N \approx Z$.

(2) With simple translational factors (e.g., plane wave phase factors, etc.), the PSS method can produce cross sections within a 20% accuracy for v up to $\sim 1v_0$, provided a basis is used which includes all the important couplings.

(3) With elaborate, optimized translational factors, cross sections can be obtained with expected accuracy better than 10% for v up to $\sim 1v_0$.

(4) The size of the basis required for total cross section calculations depends both on Z and v. For small Z, the number of important radial couplings is restricted and for small v ($\leqslant 0.05\, v_0$) the rotational coupling plays a negligible role. For large values of Z, the number of important radial couplings is large and for an accuracy of $\sim 20\%$ the basis should contain at least $N \approx Z$ states.

(5) The calculations of partial charge exchange cross sections (capture into a particular final n,ℓ-state) require much larger basis sets which, depending on the collision energy, may range from $N \approx 3Z$ to $N \approx 5Z$.

The scattering equations of the CC-MO method in the diabatic representation of molecular functions can be solved exactly under the following assumptions[14]: (1) the n- and ℓ-dependences of the coupling matrix elements are factorized; (2) the differences of the ionic diabatic potential energies do not depend on ℓ; (3) rotational coupling can be ignored. For the hydrogen atom-fully stripped ion system, these assumptions are well satisfied when $Z \gg 1$ and when the collision velocity is low ($v \lesssim 0.5v_0$). This analytical CC-MO method will be referred to as CC-MO-An.

b. Multichannel Landau–Zener (M-LZ) Model

A straightforward application of the multichannel Landau–Zener (M-LZ) model[6] to the charge exchange process in hydrogen atom-fully stripped ion system leads to a significant underestimation of the cross section in the energy region below the cross section maximum and even to an incorrect prediction of its position. This situation can be substantially improved if the rotational coupling between the degenerate Stark states in the ionic channels is taken into account (M-LZ-RC model).[15,16] A particular limitation of the M-LZ-RC model is that capture into states with $n \geqslant Z$ are not allowed (absence of pseudocrossing points). With increasing Z, however, this limitation becomes insignificant for the accuracy of total cross section calculations as well as for the partial cross sections with n close to $n_m \approx Z/2$, where n_m is the principal quantum number of the maximum populated ionic level in the charge transfer process. For $0.1 \leqslant (v/v_0) \leqslant 1$ and $0.8 \leqslant Z \leqslant 30$, the assessed accuracy of the M-LZ-RC model is $\sim 50\%$.

c. Decay Models (DM)

Decay models (DM)[7–9] assume a large number of open reaction channels for the electron capture, densely distributed in energy. The simplest version of a decay model is the absorbing sphere model (ASM).[7] The electron tunneling theories (ETT)[8,9] describe the process as decay of the atomic state due to its interaction with a quasicontinuum of final ionic states. The assumptions of the decay models are best satisfied for $0.2v_0 \leqslant v \leqslant 0.5v_0$ and for large values of Z ($\gtrsim 15$). For this region of the parameters v and Z, the accuracy of decay models is $\sim 50\%$ or better, and improves with increasing Z. Outside the above region of v and Z, the accuracy of DM calculations drops drastically.

2.2. Intermediate Collision Velocities

The treatment of the charge exchange problem at intermediate collision velocities ($v \approx 1$–$4v_0$) is difficult because no suitable expansion parameter in the theory exists for this region. An atomic orbital expansion of the total wave function and a numerical treatment of the resulting close-coupled equations seems to be the most appropriate approach to the problem (CC-AO method). Plane wave translational factors are sufficient to describe the momentum transfer effects. The important role that continuum states play in this region requires inclusion of suitable pseudostates in the expansion. It turns out, however, that a classical description of the process in this energy region is also adequate for many purposes.

a. CC-AO Method

The basis set for the CC-AO method should contain atomic orbitals centered on each of the nuclei. This is especially important for low Z-values. For the case of high Z, the basis can be reduced to a $1s$ orbital around the proton together with the orbitals around the nucleus Z representing all the important final states. For $v \gtrsim 1v_0$, there is little difference between the results of the coupled multichannel calculations and the sum of the cross sections from two-state calculations in which each final state is taken in turn. For $v < v_0$, however, at least the degenerate levels for a given n should be coupled together. The contribution from the states with $n \gtrsim Z$ can be estimated from the Oppenheimer n^{-3} rule, which reduces the size of the CC-AO calculations. The most extensive CC-AO cross section calculations have been carried out for He^{2+} (Refs. 17–19) and C^{6+} (Ref. 20).

The lower velocity limit of the validity region of the CC-AO method is not known. It is certainly valid down to $v = 0.2v_0$, and good agreement between CC-MO and CC-AO calculations has been reported for C^{6+} for velocities down to $v = 0.03v_0$.[20] At high velocities, the continuum intermediate states become increasingly important, and this requires the introduction of pseudostates into the basis. Without the inclusion of pseudostates, the use of the CC-AO method can be extended up to $v \approx 3 - 4v_0$. The one and one-half center expansion,[21] which employs a large basis on the ionic center with a simplified description of H($1s$) channel, appears to give a good account of both ionization and charge exchange and promises to provide a practical method of calculating without any definite upper velocity limit.

Like in the CC-MO method, the calculations of the partial (n,ℓ) cross sections by the CC-AO method require a much larger basis set than for the total cross section calculations.

b. Approximate Treatment of CC-AO Equations

A sufficient basis for the charge exchange problem in the hydrogen atom-fully stripped ion system can be obtained by taking only the H($1s$) orbital together with a complete set of orbitals representing the final (ionic) states.[4] The set of equations formed from this basis can be approximated either by the unitarized distorted wave approximation (UDW),[22–24] or by an approximate analytical solution, ignoring the second and higher order transition effects.[25] In the UDW approximation, the coupling matrix elements are calculated in the distorted wave Born approximation, whereas in the second, analytical approach, they are calculated in the Vainshtein–Presnyakov–Sobelman (VPS) approximation. The second method will be referred to as multichannel VPS approximation (M-VPS). Neither UDW nor M-VPS take into account coupling with the continuum and so can only be used up to $v \lesssim 3$–$4v_0$. Because the omitted second-order terms become important at low velocities, the lower limit of UDW can be assessed to be $v_{min} \simeq 0.7v_0$, whereas for the M-VPS it is around $v_{min} \simeq 0.2$–$0.3v_0$. Additional assumptions involved in M-VPS limit its application to ions with $Z \gtrsim 10$. Both these methods tend to overestimate the cross sections in the regions outside of those specified above.

c. Classical Methods

Classical dynamics can also be used to calculate the charge exchange cross section in the intermediate velocity region. The classical three-body problem can be solved numerically (using the Monte Carlo method) by making a random selection of the initial conditions.[26] This method, called classical-trajectory Monte Carlo method (CTMC), is able to provide both total and partial cross sections. Partly because of the difficulty of obtaining statistically meaningful results, the upper velocity limit of the CTMC method is about $v_{max} \simeq 3v_0$, while below $v_{min} \simeq v_0$, molecular effects may become important. The method requires high Z-values, for which capture into high n levels is dominant and for which the classical picture is more appropriate.

A second classical model has been developed to describe the over-barrier electron transitions in the $H + Z$ system.[27] For $v \lesssim v_0$ approximate analytical solution of the classical transition probability can be obtained and the model is therefore denoted by Cl M-An. Since the assumption of the adiabatic motion of the nuclei is incorporated in Cl M-An, its upper velocity limit is $v_{max} \simeq v_0$, whereas the lower limit $v_{min} \simeq 0.5v_0$ is imposed by the important quantum barrier penetration effects. High values of Z are required ($Z \gtrsim 15$) in the Cl M-An model in order to obtain over-barrier transitions in the $H + Z$ system at $v \lesssim 1v_0$.

The accuracy obtained by the CTMC method is surprisingly high, while the Cl M-An model is less successful and tends to overestimate the cross section by a factor up to 1.5.

2.3. High Velocity Region

In the energy region under consideration, first-order perturbation methods for the $H + Z$ charge exchange problem are completely inaccurate (sometimes by an order of magnitude). At much higher velocities, outside our region of interest, second-order perturbation theory provides the leading contribution to the cross section, but in the region of interest it is likely that at least five or six terms in the perturbation series are required. It follows that methods which take into account the important higher order effects must be used. The accuracy of first-order method(s) [such as the first-Born approximation (B1), Jackson–Schiff (JS) approximation, Coulomb–Born (CB) approximation, etc.] cannot be specified in any meaningful way.

a. The Brinkmann–Kramers and Eikonal Approximations

The first-order term in the perturbation series for charge exchange, omitting the internuclear potential, provides the Brinkmann–Kramers (BK) approximation. Although an inadequate approximation in itself, it appears to provide moderately accurate cross section ratios. At a given velocity, this ratio is

$$\frac{\sigma(n)}{\sigma(n_0)} = \left(\frac{n_0}{n}\right)^3, \quad n > n_0, \tag{2}$$

and becomes more accurate for large n_0, with $n > n_0$. This expression, known as Oppenheimer's n^{-3} rule, is often used to extrapolate the results obtained by some other method for the states with $n \leqslant n_0$, in the region $n > n_0$. A good accuracy of Eq. (2) is achieved for $n_0 \gtrsim Z$.

By representing the total wave function by an eikonal (Glauber) approximation and using this function in the exact T-matrix element for the transition, all higher order terms in the Born series are allowed for approximately. For the $H(1s) + Z$ system the cross section in this approximation (BK-Eik) for capture into the nth shell[28–30] is

$$\sigma_{\mathrm{Eik}}^{\mathrm{BK}}(n) = \alpha(n,Z,v)\sigma^{\mathrm{BK}}(n), \tag{3}$$

where $\alpha(n,Z,v)$ is a scaling function, weakly dependent on n and Z, but relatively strongly dependent on v. For $2v_0 \leqslant v \leqslant 5v_0$, α varies smoothly between 0.15 and 0.4. The cross section for capture into individual $(n\ell)$ levels can also be obtained.

The BK-Eik method appears to provide reasonably accurate cross sections for $2v_0 \leqslant v \leqslant 7v_0$.

b. The Continuum Distorted Wave and Related Models

In the continuum distorted wave (CDW) approximation (see, e.g., Ref. 31), the interaction in the initial state, between the incident nucleus and the bound electron, is represented by a Coulomb function; a similar approximation is made in the wave function representing the final state. The approximate transition matrix element includes contributions to all higher order terms of the perturbation series and, in particular, an important part of the second-order term. It provides very accurate results for the $(H + Z)$ system for $v > 2.5v_0$, and in the limit $v \to \infty$, it is practically equivalent to the second-Born approximation. Each partial cross section is calculated separately and summed to provide the total cross section. Although the n^{-3} rule is often used in conjunction with the CDW method, it has not been deduced from the method, but it has been justified within the second-Born approximation for $n \gg 1$.[32] The impulse approximation has also been applied in the high-energy region, but in general is less satisfactory than the CDW model.

2.4. Resumé of the Regions of Validity and Accuracies of Theoretical Methods

The preceding analysis of the theoretical methods used for charge exchange cross section calculations in the hydrogen atom-fully stripped ion system shows that two dynamical parameters determine the region of applicability of a particular method: the relative velocity v and the ionic charge Z. Also, some of the methods have intrinsic limitations due to the character of the approximations involved, while other methods (mainly based on MO or AO expansions) are limited only by the computer time constraints. In order to classify the methods by the accuracy of their cross section results, we introduce the following categories of accuracy:

Category	Accuracy
(a)	Better than + 20%
(b)	± 20%–± 50%
(c)	± 50%–± 100%
(d)	Worse than 100%

The discussion on the validity region and accuracy of different methods is summarized in Table 1.

3. Review of Data Sources

The most extensive studies of the charge exchange collision between hydrogen atom and completely stripped, multicharged ions began about ten years ago. In the previous period, cross section calculations have been performed for low-Z ions (particularly for He^{2+}), which subsequently have been superseded by more elaborate calculations within the same method. Moreover, the earlier data are presented in several review papers.[33,34] Therefore, we have chosen to compile and analyze the cross section data sources starting from 1973. The information contained in these sources is presented in Table 2. For each of the fully stripped ions with charges between $Z = 2$ and $Z = 54$ (W^{74+} is also included for completeness), the energy range, the applied method, and the character of the data (total or partial cross sections, or both) are indicated. In some cases, the applied method or the performed calculations are supplemented by comments which, together with the accuracy assessments of the methods given in Table 1, may help in the estimation of accuracy of the data. In Table 2, we do not assign the degree of accuracy of the data, since many of them are performed beyond the validity region of the applied method. Moreover, a more precise evaluation of the data accuracy requires inclusion of some other criteria, and this will be done in the next section.

4. Criteria for Evaluation of the Cross Section Data

The evaluation of the accuracy of the theoretical cross section data specified in Table 2 has been carried out on the

basis of the following criteria:

(1) degree of sophistication of the calculations within a given method (e.g., number of coupled states and the character of translational factors in CC methods, number of channels included in the multichannel methods, account of different couplings in the calculations, etc.);

(2) degree of the intrinsic accuracy of the method itself, as specified in Table 1;

(3) agreement with the most accurate experimental data for cases where such data exist.

It should be immediately noted that the experimental charge exchange data for hydrogen atom-fully stripped ion systems are extremely scarce. Only for the $H + He^{2+}$ case (and to a lesser extent, for the $H + Li^{3+}$ case) do data exist in a broad energy region ($\sim$1–200 keV/u). For B^{5+} experimental data are restricted in the energy region from $\sim$80 to 250 keV/u, and for C^{6+} they are available in the regions $\sim$0.3–3.5 keV/u and $\sim$100–200 keV/u. For the ions N^{7+} and O^{8+}, experimental data are available only at restricted energies. The experimental sources which were used for data comparison are Refs. 42 and 76–84. The lack of sufficient experimental data has forced us to assess the accuracy of the cross section data mainly on the pure theoretical criteria (1) and (2). When applying these criteria to the data listed in Table 2, only the energy ranges which conform with the validity region of the corresponding method, employed in the calculations, were considered.

5. Evaluated Cross Section Data

5.1. Total Cross Sections

We have applied the criteria discussed in the last paragraph to evaluate all the total cross section data listed in Table 2. For those reactions for which comparison with experimental data is possible, the best agreement is obtained with the results of the large-basis close-coupling calculations (in the low and medium energy range) and with the results of CTMC calculations (in the region 30–200 keV/u).

The evaluated total cross section data having an accuracy (a) or (b) are listed in Table 3, together with the energy range in which that accuracy has been attained. The data presented in this table may be considered as the best available at present and are recommended for use in practical applications. The cross section data for this list for $2 \leqslant Z \leqslant 14$ and $Z = 18$, 20, 26, 30, 36, 42, and 74 are presented graphically in Figs. 1–20. The data for all Z are given in Table 4. In order to cover as wide an energy region as possible in the figures and table, we have also included data which fall in the accuracy category (c). In presenting these data, we have adopted the following criteria:

From all the available calculations using the same method, only those with highest accuracy are presented;

If several methods provide data in a given energy range, only those with highest accuracy are presented.

The cross sections of the M-LZ-RC model[16,71] for all $Z \geqslant 16$ and in the energy range from $4 \cdot 10^{-2}$ to 10^2 keV/u ($0.004\, v_0 \leqslant v \leqslant 2v_0$) can be represented by the formula

$$\sigma = 2.25Z \ln\left(\frac{15v_0}{v}\right) \times 10^{-16}\ \text{cm}^2, \tag{4}$$

within an accuracy of 5%.

From our analysis of the existing cross section data, the following methods can be recommended for high accuracy cross section calculations [category (a)]:

(1) Energy region below 25 keV/u:
PSS method with a large MO-basis ($N \sim (2-3)Z$) and appropriate translational factors.

(2) Energy region $\sim$10–400 keV/u:
CC-AO method with a large basis ($N \approx 5Z$) and plane wave translational factors.

(3) Energy region above $\sim$400 keV/u:
CDW method, applied separately to a large number of final states [up to the principal shell $n \approx (Z + 3)$] and the use of the n^{-3} scaling afterwards.

5.2. Partial Cross Sections

Only the partial cross sections for electron capture into a given final principal shell $n(\sigma_n)$ have been evaluated using the same criteria as for the total capture cross sections. The uncertainties of the $\sigma_{n\ell}$ and $\sigma_{n\ell m}$ partial cross sections are at present high, and only a restricted number of them can be recommended for use. Generally, for most of the partial cross section data, the accuracy attained is lower than for the total cross section. This holds especially for the results provided by the M-LZ-RC, UDW, CTMC methods. The expansion methods (CC-MO and CC-AO) with large basis sets and the CDW method are able to produce the most reliable partial cross sections in the energy region of their validity.

Most of the partial cross section data have been produced by the M-LZ-RC, UDW, and CTMC methods. The accuracy of σ_n data obtained by M-LZ-RC is in the category (b) when $n \sim Z/2$ and decreases rapidly when in the difference $|n - (Z/2)|$ increases. The UDW method gives results of accuracy (b) for σ_n and $\sigma_{n\ell}$ when the collision velocity is close to $v \approx 1$–$2v_0$. The accuracy of CTMC σ_n cross section data is highest when n is sufficiently large. The evaluation of the partial cross section data meets some difficulties due to the lack of experimental information and because of the absence of clear theoretical criteria in assessing σ_n for many of the theoretical methods. We have, therefore, decided to present the existing information on σ_n in a slightly condensed form. The data for $\sigma_{n\ell}$ for He^{2+} are presented graphically in Figs. 21–24. For A^{Z+} ions (with $Z \leqslant 12$), the existing σ_n data are presented in tabular form in Table 5, and for ions with $Z \geqslant 13$, σ_n data are presented in Figs. 25–35.

Table 1. Validity Regions and Accuracy of Different Theoretical Methods for Charge Exchange

Method	Velocity Range (v_0)	Z-region	Comments	Accuracy
			A. Low-energy methods	
1) PSS	0.01-0.5	all	- classical treatment of of nuclear motion - translational factors optional	depends on the size of the basis
	0.5-1	all	- classical treatment of nuclear motion - translational factors necessary	same as above
2) CC-MO-An	0.02-0.5	$\gtrsim$10	- analytic model - all states included - radial coupling only - no translational factors	(b) or (c)
3) M-LZ	0.02-0.5	$\gtrsim$5	- radial coupling only - no translational factors	(c) or (d), $v \lesssim 0.3$ (b) or (c), $v \gtrsim 0.3$
4) M-LZ-RC	0.02-0.5	$\gtrsim$5	- rotational coupling within given n included - no translational factors	(b), $v \gtrsim 0.1$, $6 \lesssim Z \lesssim 30$ (c) or (d), otherwise (b) or (c), $v \gtrsim 0.1$, $Z \lesssim 10$
5) ASM	0.2-0.6	$\gtrsim$14	- no rotational coupling	overestimates σ; (b) or (c), smaller v, high Z; (d), higher v, low Z
6) DM	0.2-0.6	same	same	same
			B. Intermediate-energy methods	
1) CC-AO	0.2-~3-4	all	- plane wave or Coulomb translational factors necessary	depends on number of close coupled states
2) M-VPS	0.3-~3-4	$\gtrsim$10	- unitarity preserved	(b) or (c), $v \lesssim 2$ (d), $v > 2$
3) UDW	0.7-~3-4	all	- unitarity preserved	same
4) CTMC	1-~3-4	all		(a) or (b), $Z > 6$ (c), $Z \lesssim 6$
5) Cℓ M-An	0.5-1	$\gtrsim$10		(b) or (c)
			C. High-energy methods	
1) BK	>2	all	- nucleus-nucleus interaction excluded - incorrect asymptotic v-behavior of σ	(d), overestimates σ by a factor of 3 to 10
2) BI JS, Coul-B	>2	all	- all interactions included - incorrect asymptotics	unspecified
3) DW	1-~3-4	all	- unitarity not preserved	(b) or (c), $v \lesssim 2$ (d), $v > 2.5$
4) BK-Eik	2-7	all		(b), (c)
5) CDW	$\gtrsim$4	all		(a), (b)

Table 2. Theoretical data for charge transfer between atomic hydrogen and fully stripped ions

Reference	Energy Range (keV/u)	Energy Region[a]	Method[b]	Comments	Data
			H-He^{2+}		
48	0.25-17	L	CC-MO	10-state: plane wave translational factors	$\sigma_t,\sigma_{n\ell}$
13	0.75-5	L	CC-MO		$\sigma_t,\sigma_{n\ell}$
63	0.25-5	L	CC-MO	12-state	$\sigma_t,\sigma_{n\ell}$
36	1.5-4000	M(H)	CC-AO	8-state	$\sigma_t,\sigma_{n\ell}$
37	0.25-150	(L)M	CC-AO	8- and 11-state	$\sigma_t,\sigma_n,\sigma_{n\ell}$
40	1-50	(L)M	CC-AO	no translational factors	σ_t
17	5-200	M	CC-AO	$n \leq 4$: 2-state $n > 4$: n^{-3} low	$\sigma_t,\sigma_{n\ell}$
56	2.5-250	M	CC-AO	8-state basis $n \geq 3$ by n^{-3}	$\sigma_t,\sigma_{n\ell}$
61	1.5-100	(L)M	CC-AO		$\sigma_t,\sigma_{n\ell}$
68	25-110	M	CC-AO		$\sigma_t,\sigma_{n\ell}$
70	1-50	(L)M	CC-AO	plane wave factors (a) 8-state atomic (b) 19-24 Sturmian states	σ_t
73	3.5-220	M	CC-AO	20-state basis for $n \leq 3$	$\sigma_t,\sigma_{n\ell}$
74	3.5-220	M	CC-AO	2-state for $n = 4$ n^{-3} rule for $n \geq 5$	$\sigma_t,\sigma_{n\ell}$
22	0.025-200	(L)M	UDW		σ_t
42	20-180	M	CTMC		σ_t
46	100	(M)H	BK		$\sigma_{n\ell}$
46	100	(M)H	B1		$\sigma_{n\ell}$
54	25-2000	(M)H	B1	5-state with variational translational factor	$\sigma_t,\sigma_{n\ell}$
55	6-200	(M)H	DW		$\sigma_{n\ell}$
59	130	(M)H	B2		σ_t,σ_n
35	6-750	(M)H	CDW		$\sigma_t,\sigma_{n\ell}$
38	25-500	(M)H	CDW		$\sigma_t,\sigma_{n\ell}$
39	625	H	CDW		$\sigma_{n\ell}$
58	132	(M)H	CDW	capture into $1 \leq n \leq 15$ to illustrate departure from n^{-3} rule	σ_n
			H-Li^{3+}		
57	1-6	L	CC-MO	5 states no translational factors	σ_t
17	5-200	M	CC-AO	$n \leq 4$, 2-state $n > 4$, n^{-3} low	σ_t,σ_n
67	1.4-200	(L)M	CC-AO	$n \leq 3$, 20 states $n = 4$, 2 states $n > 4$, n^{-3} rule	σ_t,σ_n
72	50,100,200	M	CC-AO		σ_n
23	0.02-200	(L)M	UDW		σ_t
69	0.01-5000	(L)M(H)	UDW	includes ionization channel	σ_t
40	37.5-140	M	CTMC		σ_t
26	37.5-140	M	CTMC		σ_t
65	50	M	CTMC		$\sigma_t,\sigma_n,\sigma_{n\ell}$

Table 2. Theoretical data for charge transfer between atomic hydrogen and fully stripped ions--Continued

Reference	Energy Range (keV/u)	Energy Region[a]	Method[b]	Comments	Data
			H-Li^{3+}		
64	14-300	(M)H	B1	1s,2s,2p,3s,3p,3d final states	$\sigma_t,\sigma_{n\ell}$
53	1.3-258	(L)(M)H	BK-Eik	n = 1-7 separately $n \geq 8$, n^{-3} rule	σ_t
60	30-1000	(M)H	BK-Eik		σ_t
59	130	(M)H	B2		σ_t,σ_n
39	625	H	CDW		$\sigma_{n\ell}$
31	28.6-286	(M)H	CDW	n = 1-3, separately $n \geq 4$, n^{-3} rule	σ_t
53	1.3-258	L(M)H	CDW		σ_t
58	132	(M)H	CDW	capture into $1 \leq n \leq 15$ to illustrate departure from n^{-3} rule	σ_n
			H-Be^{4+}		
41	0.1-20.3	L	PSS	3 molecular states no rotational coupling plane wave translational factors	σ_t
7	2.58	L	ASM		σ_t
45	1-100	L(M)	DM		σ_t
40	1-130	M	CC-AO	sequence of 2-state CC; unphysical oscillations; plane wave translational factors	σ_t
17	5-200	M	CC-AO	$n \leq 5$; 2-st cc $n > 5$; n^{-3} low	σ_t,σ_n
23	0.02-200	(L)M	UDW		σ_t
26	37.5-140	M	CTMC		σ_t
65	50,100	M	CTMC		$\sigma_t,\sigma_n,\sigma_{n\ell}$
46	100	(M)H	BK	$n \leq 10$	$\sigma_{n\ell}$
46	100	(M)H	B1		$\sigma_{n\ell}$
59	130	(M)H	B2		σ_t,σ_n
39	625	H	CDW		$\sigma_{n\ell}$
58	132	(M)H	CDW	capture into $1 \leq n \leq 15$ to illustrate departure from n^{-3} rule	σ_n
			H-B^{5+}		
41	0.25-25	L	PSS	3-states	σ_t
23	0.05-8	L	PSS		σ_t
66	0.5,1	L	CC-MO-An	n,ℓ - separable interaction model	σ_t
16	0.49,1,10,25	L	M-LZ-RC	rotational coupling included	$\sigma_t,\sigma_{n\ell}$
7	2.58	L	ASM		σ_t
45	1-100	L(M)	DM		σ_t
9	2.58,47.3	L(M)	DM		σ_t
40	1-170	M	CC-AO	sequence of two-state CC	σ_t
17	5-200	M	CC-AO	$n \leq 5$, 2-state CC $n > n^{-3}$ low	$\sigma_t,\sigma_n,\sigma_{n\ell}$
23	0.02-200	(L)M	UDW		σ_t

Table 2. Theoretical data for charge transfer between atomic hydrogen and fully stripped ions--Continued

Reference	Energy Range (keV/u)	Energy Region[a]	Method[b]	Comments	Data
			H-B^{5+}		
69	0.01-5000	(L)M(H)	UDW		σ_t
26	37.5-150	M	CTMC		σ_t
49	25,32,55,73	M	CTMC		$\sigma_t,\sigma_n,\sigma_{n\ell}$
65	50	M	CTMC		$\sigma_t,\sigma_n,\sigma_{n\ell}$
59	130	(M)H	B2		σ_t,σ_n
39	625	H	CDW		$\sigma_{n\ell}$
58	132	(M)H	CDW	capture into $1 \leq n \leq 15$ to illustrate departure from n^{-3} rule	σ_n
			H-C^{6+}		
52	0.0625-25	L	CC-MO		σ_t
10	0.013-27.4	L	CC-MO	translational factors included nonlinear trajectories below 1.3 keV/u	$\sigma_t,\sigma_n,\sigma_{n\ell}$
43	0.05-20	L	PSS	6 molecular states; coord. origin on H^+ rotational coupling included	σ_t
44	0.0625-6.25	L	PSS	11 states; (adiabatic molecular) rotational coupling included Coulomb trajectories for; nuclei; R-adjustable translational factors	σ_t
66	0.5,1	L	CC-MO-An	n,ℓ - separable interaction model	σ_t
6	0.04-2.8	L	M-LZ	rotational coupling excluded	σ_t
15	0.01-25	L	M-LZ-RC	rotational coupling included	σ_t
16	0.04-50	L	M-LZ-RC		$\sigma_t,\sigma_n,\sigma_{n\ell}$
71	0.1,1,10	L	M-LZ-RC		σ_t,σ_n
7	2.58	L	ASM		σ_t
45	1-100	L(M)	DM		σ_t
9	2.58,47.3	L(M)	DM		σ_t
40	1-180	M	CC-AO	sequence of two-state CC	σ_t
20	0.1-1	(L)M	CC-AO	curved line trajectory	σ_t
23	0.02-2000	(L)M(H)	UDW		σ_t
69	0.01-5000	(L)M(H)	UDW	includes ionization and excitation channels	σ_t
26	37.5-150	M	CTMC		σ_t
43	20-200	M	CTMC		σ_t
49	25,33,55,76	M	CTMC		$\sigma_t,\sigma_n,\sigma_{n\ell}$
65	25,50,75,100	M	CTMC		$\sigma_t,\sigma_n,\sigma_{n\ell}$
47	50,500,5000	(M)H	BK-Eik		σ_n
62	40-200	(M)H	BK-Eik		$\sigma_t,\sigma_n,\sigma_{n\ell}$
59	130	(M)H	B2		σ_t,σ_n
39	500-5000	H	CDW		$\sigma_{n\ell}$
58	132	(M)H	CDW	capture into $1 \leq n \leq 15$ to illustrate departure from n^{-3} rule	

Table 2. Theoretical data for charge transfer between atomic hydrogen and fully stripped ions--Continued

Reference	Energy Range (keV/u)	Energy Region[a]	Method[b]	Comments	Data
			H-N^{7+}		
66	0.5;1	L	CC-MO-An	(n,ℓ) separable interaction model	σ_t
6	0.028-2.8	L	M-LZ	rotational coupling excluded	σ_t
16	0.49,1,10,25	L	M-LZ-RC	rotational coupling included	σ_t,σ_n
71	0.01-100	L(M)	M-LZ-RC	rotational coupling included	σ_t
7	2.58	L	ASM		σ_t
45	1-100	L(M)	DM		σ_t
9	2.58,47.3	L(M)	DM		σ_t
40	1-200	M	CC-AO	sequence of 2-state CC	σ_t
26	37.5-150	M	CTMC		σ_t
65	50	M	CTMC		$\sigma_t,\sigma_n,\sigma_{n\ell}$
39	625	H	CDW		$\sigma_{n\ell}$
			H-O^{8+}		
66	0.5,1	L	CC-MO	(n,ℓ) separable interaction model	σ_t
75	0.01-35	L	CC-MO	33 states	$\sigma_t,\sigma_n,\sigma_{n\ell}$
41	0.25-25	L	PSS	3-molecular states + rotational coupling; origin on O^{8+}	σ_t
50	0.025-7.56	L	PSS	8-molecular states + rotational coupling; origin on O^{8+} origin on H^+	σ_t
6	0.028-2.8	L	M-LZ	no rotational coupling	σ_t
15	0.01-25	L	M-LZ-RC	rotational coupling included	σ_t
16	0.01-50	L	M-LZ-RC		$\sigma_t,\sigma_n,\sigma_{n\ell}$
71	0.1,1,10	L(M)	M-LZ-RC		σ_t,σ_n
7	2.58	L	ASM		σ_t
45	1-100	L(M)	DM		σ_t
9	2.58,47.3	L(M)	DM		σ_t
40	1-180	M	CC-AO	sequence of 2-state CC	σ_t
22	0.02-200	(L)M	UDW		σ_t
26	37.5-150	M	CTMC		σ_t
49	25,32,55,76	M	CTMC		$\sigma_t,\sigma_n,\sigma_{n\ell}$
50	25-900	M(H)	CTMC		σ_t
65	50;100	M	CTMC		$\sigma_t,\sigma_n,\sigma_{n\ell}$
27	0.5-100	M	ClM-An		σ_t
30	100	(M)H	BK-Eik		$\sigma_{n\ell}$
62	40-200	(M)H	BK-Eik		$\sigma_t,\sigma_n,\sigma_{n\ell}$
39	625	H	CDW		$\sigma_{n\ell}$
			H-F^{9+}		
66	0.5,1	L	CC-MO-An	n,ℓ - separable interaction model	σ_t
16	0.49,1,10,25	L	M-LZ-RC	rotational coupling included	σ_t,σ_n
71	0.01-100	L(M)	M-LZ-RC		σ_t
7	2.58	L	ASM		σ_t

Table 2. Theoretical data for charge transfer between atomic hydrogen and fully stripped ions--Continued

Reference	Energy Range (keV/u)	Energy Region[a]	Method[b]	Comments	Data
			H-F^{9+}		
45	1-100	L(M)	DM		σ_t
9	2.58,47.3	L(M)	DM		σ_t
40	1-225	M	CC-AO	sequence of 2-state CC	σ_t
65	50	M	CTMC		$\sigma_t,\sigma_n,\sigma_{n\ell}$
7	625	H	CDW		$\sigma_{n\ell}$
			H-Ne^{10+}		
66	0.5,1	L	CC-MO-An		σ_t
6	0.028-2.8	L	M-LZ	rotational coupling excluded	σ_t
16	0.49,1,10,25	L	M-LZ-RC	rotational coupling included	$\sigma_t,\sigma_n,\sigma_{n\ell}$
71	0.01-100	L(M)	M-LZ-RC		σ_t,σ_n
7	2.58	L	ASM		σ_t
8	50	L(M)	DM		σ_t
45	1-100	L(M)	DM		σ_t
9	0.002-337	L(M)	DM		σ_t
25	0.01-1600	(L)M(H)	CC-AO	VPS approximation for 2-state amplitudes	σ_t
40	1-225	M	CC-AO		σ_t
24	5-2000	(L)M(H)	UDW		$\sigma_t,\upsilon_n,\sigma_{n\ell}$
26	37.5-200	M	CTMC		σ_t
65	50,100	M	CTMC		$\sigma_t,\sigma_n,\sigma_{n\ell}$
27	0.5-100	(L)M	ClM-An		σ_t
39	625	H	CDW		$\sigma_{n\ell}$
			H-Na^{11+}		
66	0.5,1	L	CC-MO-An	n,ℓ - separable interaction model	σ_t
16	0.5,1	L	M-LZ-RC	rotational coupling included	σ_t,σ_n
71	0.1,1,10	L(M)	M-LZ-RC		σ_t
7	2.58	L	ASM		σ_t
45	1-100	L(M)	DM		σ_t
9	2.58,47.3	L(M)	DM		σ_t
39	625	H	CDW		$\sigma_{n\ell}$
			H-Mg^{12+}		
66	0.5,1	L	CC-MO-An		σ_t
16	0.49,1,10,25	L	M-LZ-RC	rotational coupling included	σ_t,σ_n
71	0.1,1,10	L(M)	M-LZ-RC		σ_t
7	2.58	L	ASM		σ_t
45	1-100	L(M)	DM		σ_t
9	2.58,47.3	L(M)	DM		σ_t
40	1-225	M	CC-AO		σ_t
65	100	M	CTMC		$\sigma_n,\sigma_{n\ell}$
39	625	H	CDW		$\sigma_{n\ell}$

Table 2. Theoretical data for charge transfer between atomic hydrogen and fully stripped ions--Continued

Reference	Energy Range (keV/u)	Energy Region[a]	Method[b]	Comments	Data
			H-Al^{13+}		
66	0.5,1	L	CC-MO-An		σ_t
16	0.5,1	L	M-LZ-RC	rotational coupling included	σ_t,σ_n
71	0.01-100	L(M)	M-LZ-RC		σ_t,σ_n
7	2.58	L	ASM		σ_t
45	1-100	L(M)	DM		σ_t
9	2.58,47.3	L(M)	DM		σ_t
39	625	H	CDW		$\sigma_{n\ell}$
			H-Si^{14+}		
66	0.1-350	L(M)	CC-MO-An		σ_t
6	0.028-2.8	L	M-LZ	rotational coupling excluded	σ_t
16	0.01-50	L	M-LZ-RC	rotational coupling included	$\sigma_t,\sigma_n,\sigma_{n\ell}$
71	0.01-100	L(M)	M-LZ-RC		σ_t
7	2.58	L	ASM		σ_t
45	1-100	L(M)	DM		σ_t
9	2.58,47.3	L(M)	DM		σ_t
40	1-225	M	CC-AO		σ_t
24	5-2000	(L)M(H)	UDW		σ_n
69	0.01-5000	(L)M(H)	UDW		σ_t
26	37.5-200	M	CTMC		σ_t
65	100	M	CTMC		$\sigma_n,\sigma_{n\ell}$
27	0.5-100	(L)M	ClM-An		σ_t
39	625	H	CDW		$\sigma_{n\ell}$
			H-P^{15+}		
66	0.5,1	L	CC-MO-An		σ_t
16	0.84	L	M-LZ-RC		σ_t
71	0.1,1,10	L	M-LZ-RC		σ_t
7	2.58	L	ASM		σ_t
45	1-100	L(M)	DM		σ_t
9	2.58,47.3	L(M)	DM		σ_t
39	625	H	CDW		$\sigma_{n\ell}$
			H-S^{16+}		
66	1	L	CC-MO-An		σ_t
16	0.5,1	L	M-LZ-RC		σ_t,σ_n
71	0.1,1,10	L	M-LZ-RC		σ_t
7	2.58	L	ASM		σ_t
45	1-100	L(M)	DM		σ_t
9	2.58,47.3	L(M)	DM		σ_t
40	1-225	M	CC-AO		σ_t
65	100	M	CTMC		$\sigma_t,\sigma_n,\sigma_{n\ell}$
39	625	H	CDW		$\sigma_{n\ell}$

Table 2. Theoretical data for charge transfer between atomic hydrogen and fully stripped ions--Continued

Reference	Energy Range (keV/u)	Energy Region[a]	Method[b]	Comments	Data
			H-Cl^{17+}		
66	1	L	CC-MO-An		σ_t
71	0.01-100	L	M-LZ-RC		σ_t
7	2.58	L	ASM		σ_t
45	1-100	L(M)	DM		σ_t
9	2.58,47.3	L(M)	DM		σ_t
39	625	H	CDW		$\sigma_{n\ell}$
			H-Ar^{18+}		
66	1	L	CC-MO-An		σ_t
6	0.028-2.8	L	M-LZ		σ_t
16	0.5,1,10,25	L	M-LZ-RC		σ_n
71	0.01-100	L(M)	M-LZ-RC		σ_t
7	2.58	L	ASM		σ_t
45	1-100	L(M)	DM		σ_t
9	2.58,47.3	L(M)	DM		σ_t
40	1-225	M	CC-AO		σ_t
26	37.5-200	M	CTMC		σ_t
65	100	M	CTMC		$\sigma_t,\sigma_n,\sigma_{n\ell}$
27	0.5-100	(L)M	C1M-An		σ_t
39	625	H	CDW		$\sigma_{n\ell}$
			H-K^{19+}		
66	1	L	CC-MO-An		σ_t
71	0.01-10	L	M-LZ-RC		σ_t
7	2.58	L	ASM		σ_t
45	1-100	L(M)	DM		σ_t
9	2.58	L(M)	DM		σ_t
39	625	H	CDW		$\sigma_{n\ell}$
			H-Ca^{20+}		
66	0.05-500	L(M)	CC-MO-An		σ_t
16	0.5,1	L	M-LZ-RC		σ_n
71	0.01-100	L(M)	M-LZ-RC		σ_t
7	2.58	L	ASM		σ_t
8	50	L(M)	DM		σ_t
45	1-100	L(M)	DM		σ_t
9	0.02-300	L(M)	DM		σ_t
25	0.01-2000	(L)M(H)	CC-AO	VPS approximation for 2-state coupling	σ_t
65	100	M	CTMC		$\sigma_t,\sigma_n,\sigma_{n\ell}$
24	0.1-10	(L)M	UDW		σ_t
39	625	H	CDW		$\sigma_{n\ell}$

Table 2. Theoretical data for charge transfer between atomic hydrogen and fully stripped ions--Continued

Reference	Energy Range (keV/u)	Energy Region[a]	Method[b]	Comments	Data
			H-Sc^{21+}		
66	0.5,1	L	CC-MO-An		σ_t
71	0.5,1,10	L	M-LZ-RC		σ_t
7	2.58	L	ASM		σ_t
45	1-100	L(M)	DM		σ_t
9	2.58,45.3	L(M)	DM		σ_t
39	625	H	CDW		$\sigma_{n\ell}$
			H-Ti^{22+}		
66	0.5,1	L	CC-MO-An		σ_t
71	0.01-100	L(M)	M-LZ-RC		σ_t,σ_n
7	2.58	L	ASM		σ_t
45	1-100	(M)	DM		σ_t
9	2.58,47.3	(M)	DM		σ_t
39	625	H	CDW		$\sigma_{n\ell}$
			H-V^{23+}		
66	0.5,1	L	CC-MO-An		σ_t
71	0.5,1,10	L	M-LZ-RC		σ_t
7	2.58	L	ASM		σ_t
45	1-100	L(M)	DM		σ_t
9	2.58,47.3	L(M)	DM		σ_t
39	625	H	CDW		$\sigma_{n\ell}$
			H-Cr^{24+}		
66	0.5,1	L	CC-MO-An		σ_t
16	0.4,100	L(M)	M-LZ-RC		σ_t,σ_n
71	0.01-100	L(M)	M-LZ-RC		σ_t,σ_n
7	2.58	L	ASM		σ_t
45	1-100	L(M)	DM		σ_t
9	2.58,47.3	L(M)	DM		σ_t
39	625	H	CDW		$\sigma_{n\ell}$
			H-Mn^{25+}		
66	0.5,1	L	CC-MO-An		σ_t
71	0.1,1,10	L	M-LZ-RC		σ_t
7	2.58	L	ASM		σ_t
45	1-100	L(M)	DM		σ_t
9	2.58,47.3	L(M)	DM		σ_t
39	625	H	CDW		$\sigma_{n\ell}$

Table 2. Theoretical data for charge transfer between atomic hydrogen and fully stripped ions--Continued

Reference	Energy Range (keV/u)	Energy Region[a]	Method[b]	Comments	Data
			H-Fe^{26+}		
51	0.21,1.3,5.3	L	PSS	17-state	σ_t
66	0.5,1	L	CC-MO-An		σ_t
16	1,10,25	L	M-LZ-RC		σ_n
71	0.01-100	L(M)	M-LZ-RC		σ_t,σ_n
7	2.58	L	ASM		σ_t
45	1-100	L(M)	DM		σ_t
9	2.58,47.3	L(M)	DM		σ_t
27	0.5-100	L	ClM-An		σ_t
26	37.5-200	M	CTMC		σ_t
51	84-258	M	CTMC		σ_t
39	625	H	CDW		$\sigma_{n\ell}$
			H-Co^{27+}		
66	0.5,1	L	CC-MO-An		σ_t
71	0.1,1,10	L	M-LZ-RC		σ_t
7	2.58	L	ASM		σ_t
45	1-100	L(M)	DM		σ_t
9	2.58,47.3	L(M)	DM		σ_t
39	625	H	CDW		$\sigma_{n\ell}$
			H-Ni^{28+}		
66	0.5,1	L	CC-MO-An		σ_t
16	10,25	L	M-LZ-RC		σ_n
71	0.01-100	L(M)	M-LZ-RC		σ_t,σ_n
7	2.58	L	ASM		σ_t
45	1-100	L(M)	DM		σ_t
9	2.58,47.3	L(M)	DM		σ_t
39	625	H	CDW		$\sigma_{n\ell}$
			H-Cu^{29+}		
66	0.5,1	L	CC-MO-An		σ_t
81	0.01-100	L(M)	M-LZ-RC		σ_t
8	2.58	L	ASM		σ_t
45	1-100	L(M)	DM		σ_t
9	2.58,47.3	L(M)	DM		σ_t
39	625	H	CDW		$\sigma_{n\ell}$
			H-Zn^{30+}		
66	0.075-750	L(M)	CC-MO-An		σ_t
71	0.1,1,10	L	M-LZ-RC		σ_t
7	2.58	L	ASM		σ_t
8	50	L(M)	DM		σ_t

Table 2. Theoretical data for charge transfer between atomic hydrogen and fully stripped ions--Continued

Reference	Energy Range (keV/u)	Energy Region[a]	Method[b]	Comments	Data
			H-Zn^{30+}		
45	1-100	L(M)	DM		σ_t
9	0.2-337	L(M)	DM		σ_t
39	625	H	CDW		$\sigma_{n\ell}$
			H-Ga^{31+}		
71	0.1,1,10	L	M-LZ-RC		σ_t
7	2.58	L	ASM		σ_t
9	2.58,47.3	L(M)	DM		σ_t
			H-Ge^{32+}		
71	0.1,1,10	L	M-LZ-RC		σ_t
7	2.58	L	ASM		σ_t
9	2.58,47.3	L(M)	DM		σ_t
			H-As^{33+}		
71	0.1,1,10	L	M-LZ-RC		σ_t
7	2.58	L	ASM		σ_t
9	2.58,47.3	L(M)	DM		σ_t
			H-Se^{34+}		
71	0.1,1,10	L	M-LZ-RC		σ_t
7	2.58	L	ASM		σ_t
9	2.58,47.3	L(M)	DM		σ_t
			H-Br^{35+}		
71	0.1,1,10	L	M-LZ-RC		σ_t
7	2.58	L	ASM		σ_t
9	2.58,47.3	L(M)	DM		σ_t
			H-Kr^{36+}		
16	10,25	L	M-LZ-RC		σ_n
71	0.01-100	L(M)	M-LZ-RC		σ_t
7	2.58	L	ASM		σ_t
9	2.58,47.3	L(M)	DM		σ_t
26	37.5-200	M	CTMC		σ_t
27	0.5-100	(L)M	ClM-An		σ_t
			H-Rb^{37+}		
71	0.1,1,10	L	M-LZ-RC		σ_t
7	2.58	L	ASM		σ_t
9	2.58,47.3	L(M)	DM		σ_t

Table 2. Theoretical data for charge transfer between atomic hydrogen and fully stripped ions--Continued

Reference	Energy Range (keV/u)	Energy Region[a]	Method[b]	Comments	Data
			H-Sr^{38+}		
71	0.1,1,10	L	M-LZ-RC		σ_t
7	2.58	L	ASM		σ_t
9	2.58,47.3	L(M)	DM		σ_t
			H-Y^{39+}		
71	0.1,1,10	L	M-LZ-RC		σ_t
7	2.58	L	ASM		σ_t
9	2.58,47.3	L(M)	DM		σ_t
			H-Zr^{40+}		
71	0.01-100	L(M)	M-LZ-RC		σ_t
7	2.58	L	ASM		σ_t
9	2.58,47.3	L(M)	DM		σ_t
			H-Cb^{41+}		
71	0.1,1,10	L	M-LZ-RC		σ_t
7	2.58	L	ASM		σ_t
			H-Mo^{42+}		
71	0.01-100	L(M)	M-LZ-RC		σ_t,σ_n
7	2.58	L	ASM		σ_t
			H-Tc^{43+}		
71	0.1,1,10	L	M-LZ-RC		σ_t
7	2.58	L	ASM		σ_t
			H-Ru^{44+}		
71	0.1,1,10	L	M-LZ-RC		σ_t
7	2.58	L	ASM		σ_t
			H-Rh^{45+}		
71	0.1,1,10	L	M-LZ-RC		σ_t
7	2.58	L	ASM		σ_t
			H-Pd^{46+}		
71	0.1,1,10	L	M-LZ-RC		σ_t
7	2.58	L	ASM		σ_t
			H-Ag^{47+}		
71	0.1,1,10	L	M-LZ-RC		σ_t
7	2.58	L	ASM		σ_t

Table 2. Theoretical data for charge transfer between atomic hydrogen and fully stripped ions--Continued

Reference	Energy Range (keV/u)	Energy Region[a]	Method[b]	Comments	Data
			H-Cd^{48+}		
71	0.01-100	L	M-LZ-RC		σ_t
7	2.58	L	ASM		σ_t
			H-In^{49+}		
71	0.1,1,10	L	M-LZ-RC		σ_t
7	2.58	L	ASM		σ_t
			H-Sn^{50+}		
71	0.1,1,10	L	M-LZ-RC		σ_t
7	2.58	L	ASM		σ_t
			H-Sb^{51+}		
71	0.1,1,10	L	M-LZ-RC		σ_t
			H-Te^{52+}		
71	0.1,1,10	L	M-LZ-RC		σ_t
			H-I^{53+}		
71	0.1,1,10	L	M-LZ-RC		σ_t
			H-Xe^{54+}		
71	0.01-100	L(M)	M-LZ-RC		σ_t
			H-W^{74+}		
71	0.01-100	L(M)	M-LZ-RC		σ_t

[a] L, M, H stand for the low-, medium-, and high-energy regions, respectively. These letters in parentheses indicate regions in which the methods were applied, although invalid.

[b] Definition of abbreviations for methods used in table:

CC-MO	Close coupling - molecular orbital method
PSS	Perturbed stationary state method
CC-MO-An	Close-coupling molecular orbital, analytical model
M-LZ	Multichannel Landau-Zener model
M-LZ-RC	Multichannel Landau-Zener model with rotational coupling
ASM	Absorbing sphere model
DM	Decay model
CC-AO	Close coupling - atomic orbital method
M-VPS	Multichannel Vainstein-Presnyakov-Sobelman approximation
UDW	Unitarized distorted wave approximation
CTMC	Classical trajectory Monte Carlo method
Cℓ•M-An	Classical model, analytical
BK	Brinkmann-Kramers approximation
B1	First Born approximation
JS	Jackson-Schiff approximation
DW	Distorted wave approximation
BK-Eik	Brinkmann-Kramers - Eikonal approximation
B2	Second Born approximation
CDW	Continuum distorted wave approximation

Table 3. Evaluated Best Total Charge Exchange Cross Sections Data for Hydrogen Atom-Fully Stripped Ion Systems

Ion	Energy Range (keV/u)	Accuracy[a]	References
He^{2+}	0.25–500	(a) or (b)	36,38,13,48,63,70,56,73
Li^{3+}	1.5–25	(a) or (b)	67
	25–100	(a)	69
	30–140	(a) or (b)	26
	100–200	(a) or (b)	72
Be^{4+}	0.1–10	(a) or (b)	41
	1–200	(b)	26,23,17
B^{5+}	0.05–10	(a) or (b)	23,69,16
	10–200	(a) or (b)	69
	40–200	(b)	26
C^{6+}	0.013–27	(a)	10,66
	0.5–50	(a) or (b)	69,16
	25–200	(a) or (b)	69,26
N^{7+}	0.5–80	(b)	71
	37–150	(b)	26
O^{8+}	0.01–32	(a)	75
	0.02–0.8	(b) or (c)	22,50,16
	0.8–80	(b)	22,16,27
	40–150	(a) or (b)	26,22
F^{9+}	0.7–80	(b)	71
Ne^{10+}	0.8–60	(b)	71,24
	40–200	(a) or (b)	26,24
Na^{11+}, Mg^{12+}	1,10	(b)	71
	1	(b)	45,66
Al^{13+}	0.8–80	(b)	71
Si^{14+}	0.5–50	(b)	71,69
	35–200	(b)	26
P^{15+}, S^{16+}	1,10	(b)	71,16
	100	(a) or (b)	65
Cl^{17+}	0.8–70	(b)	71
Ar^{18+}	0.5–100	(b)	27,26
	40–200	(b)	26
Kr^{19+}	1,10	(b)	71
	1;2.6	(b)	45,7
Ca^{20+}	0.4–100	(b)	71
	100	(b)	65
Sc^{21+}	1,10	(b)	71
	1,2;2.6	(b)	45,7
Ti^{22+}	0.5–80	(b)	71
	1;2.6	(b)	66,7
V^{23+}	1,10	(b)	71
	1;2.6	(b)	64,45,7
Cr^{24+}	0.5–100	(b)	71
	1;2.6	(b)	
Mn^{25+}	1,10	(b)	71
	1;2.6	(b)	45,7
Fe^{26+}	0.5–100	(b)	27,71
	40–200	(b)	26
Co^{27+}	1,10	(b)	71
	1;2.6	(b)	45,66,7
Ni^{28+}, Cu^{29+}	0.5–100	(b)	17
	1;2.6	(b)	45,66,7
Zn^{30+}	0.2–10	(b)	66
	1;2.6	(b)	45,71,7
Ga^{31+}, Ge^{32+}, As^{33+} Sc^{34+}, Br^{35+}	1;2.6;10	(b)	71,7
Kr^{36+}	0.4–100	(b)	71
	3–100	(b)	27
	40–200	(b)	26
Rb^{37+}, Sr^{38+}, Y^{39+}	1;2.6;10	(b)	71,7,71
Zr^{40+}	0.4–100	(b)	71
	2.6	(b)	7
Cb^{41+}	1;2.6;10	(b)	71,7,71
Mo^{42+}	0.4–100	(b)	71
Tc^{43+}, Ru^{44+}, Rh^{45+} Pd^{46+}, Ag^{47+}	1;2.6;10	(b)	71,7,71
Cd^{48+}	0.2–100	(b)	71
In^{49+}, Sn^{50+}, Sb^{51+} Te^{52+}, I^{53+}	0.1,1,10	(b)	71
Xe^{54+}	0.1–100	(b)	71
W^{74+}	0.2–100	(b)	71

[a]Accuracies defined in section 2.4.

Table 4. Evaluated theoretical total charge exchange cross sections (σ_t) for the process $A^{Z+} + H \rightarrow A^{(Z-1)+} + H^+$ as a function of E/M, the laboratory energy of the ion divided by the mass of the ion.

E/M (keV/u)	σ_t (10^{-16} cm^2)	E/M (keV/u)	σ_t (10^{-16} cm^2)	E/M (keV/u)	σ_t (10^{-16} cm^2)	E/M (keV/u)	σ_t (10^{-16} cm^2)
H-He^{2+}						**H-Li^{3+}**	
0.25	0.26	17.6	11.0	11.4	10.4	1.4	3.89
0.75	1.49	20.7	10.4	15.9	8.87	5.	10.3
2.00	6.30	24.9	9.62	21.1	7.29	10.	16.8
5.0	12.2	27.9	8.62	32.2	5.12	25.	18.4
10.0	13.5	31.4	6.18	40.2	4.01	100.	2.11
17.5	12.1	35.3	5.88	52.2	3.00	200.	.23
Ref [48]		37.9	4.51	62.5	2.24	Ref [67]	
		40.9	3.55	79.0	1.42		
.48	.66	44.3	4.01	97.7	.755		
.56	.86	47.1	3.09	119.	.463	50.	18.2
.65	1.11	54.1	2.41	143.	.278	100.	2.67
.73	1.35	57.0	2.02	161.	.180	200.	.23
.90	1.87	60.1	2.04	183.	.108	Ref [72]	
1.20	2.97	64.9	1.59	Ref [22]			
1.53	4.24	67.5	1.29				
1.86	5.31	74.3	1.14			25.	13.5
2.17	6.17	79.7	.803	8.75	8.99	50.	6.74
2.84	8.02	85.0	.765	12.2	8.59	75.	3.25
3.11	8.69	91.5	.522	16.4	8.11	100.	1.63
3.47	9.56	94.8	.528	20.0	8.72	200.	.19
4.08	10.9	97.0	.469	24.0	8.68	Ref [69]	
4.84	12.4	100.	.414	25.0	8.88		
5.31	13.1	108.	.283	38.5	7.25		
5.98	14.3	113.	.278	44.0	5.98	35.8	10.8
7.14	16.0	Ref [68]		50.4	5.06	47.7	9.61
Ref [13]				62.4	3.04	72.8	5.00
		5.0	11.1	74.2	1.67	97.7	2.79
		17.5	11.0	85.2	1.06	123.	.75
0.25	.260	50.0	3.7	100.	1.15	Ref [26]	
0.75	1.43	Ref [70]		120.	1.03		
2.0	6.15			124.	.39		
5.00	11.2			Ref [42]		107.	1.41
Ref [63]		3.7	9.16			132.	.641
		7.5	12.6			159.	.307
		13.7	12.8	109.	.398	189.	.153
		25.5	8.48	118.	.313	Ref [53]	
		75.5	1.15	133.	.210		
		158.	.13	156.	.113		
		Ref [73]		Ref [38]			

Table 4. Evaluated theoretical total charge exchange cross sections (σ_t) for the process $A^{Z+} + H \rightarrow A^{(Z-1)+} + H^+$ as a function of E/M, the laboratory energy of the ion divided by the mass of the ion (continued).

E/M (keV/u)	σ_t (10^{-16} cm^2)	E/M (keV/u)	σ_t (10^{-16} cm^2)	E/M (keV/u)	σ_t (10^{-16} cm^2)	E/M (keV/u)	σ_t (10^{-16} cm^2)
H-Be^{4+}				**H-B^{5+}**			
0.080	12.0	5.	49.8	0.5	6.59	37.5	20.6
0.234	23.0	10.	42.4	1.0	17.4	50.	17.4
0.990	32.3	25.	31.7	Ref [66]		75.	12.9
2.33	37.3	50.	16.5			100.	6.30
2.84	38.1	100.	4.35			125.	4.62
3.55	38.8	200.	.57	0.4	8.89	150.	1.48
4.14	39.1	Ref [17]		Ref [16]		Ref [26]	
4.62	39.2						
5.24	39.2						
5.78	39.1	1.00	49.0	50.	25.3	0.050	21.7
6.25	38.8	1.34	47.3	100.	6.78	0.075	19.0
7.62	38.4	1.75	44.4	200.	.970	0.115	16.9
9.03	38.2	3.10	39.3	Ref [17]		0.173	15.6
10.8	38.4	4.49	35.7			0.292	14.4
12.3	38.4	7.90	31.2			0.385	14.1
14.0	38.7	13.7	25.4	0.5	11.9	0.616	14.5
15.8	38.9	22.7	20.8	1.0	13.9	0.936	15.5
20.0	39.8	26.0	19.7	2.5	17.8	1.15	16.1
Ref [41]		32.0	17.5	5.0	27.5	1.78	18.3
		62.0	9.21	10.	31.7	2.64	22.3
2.58	56.0	84.4	5.46	25.	26.1	3.16	25.1
Ref [7]		126.	2.14	50.	16.2	5.61	34.7
		155.	1.13	75.	9.02	7.17	39.1
1.0	49.	187.	.644	100.	4.87	Ref [23]	
2.0	47.	Ref [23]		200.	.62		
4.0	44.			Ref [69]			
8.0	42.	37.5	16.1				
10.	41.	50.	13.6				
20.	39.	75.	9.36				
Ref [45]		100.	4.61				
		125.	1.34				
		Ref [26]					

Table 4. Evaluated theoretical total charge exchange cross sections (σ_t) for the process $A^{Z+} + H \rightarrow A^{(Z-1)+} + H^+$ as a function of E/M, the laboratory energy of the ion divided by the mass of the ion (continued).

H–C^{6+}

E/M (keV/u)	σ_t (10^{-16} cm^2)
0.013	0.470
0.053	4.21
0.135	14.2
0.210	21.0
0.644	36.3
1.32	44.2
2.96	46.3
5.26	47.8
11.8	45.9
21.0	40.7
27.3	37.1
Ref [10]	
0.5	37.4
Ref [66]	
0.4	34.3
1.0	39.2
5.0	38.2
10.	35.5
25.	30.8
Ref [16]	
0.100	11.8
0.142	16.3
0.221	22.7
0.318	29.4
0.562	36.2
1.00	40.3
Ref [20]	
0.5	49.2
1.0	50.6
2.5	46.8
5.	43.1
10.	39.4
25.	32.0
50.	21.7
100.	6.92
200.	0.934
Ref [69]	
37.5	25.6
50.	22.1
75.	18.2
100.	10.3
125.	5.72
150.	1.83
Ref [26]	

H–N^{7+}

E/M (keV/u)	σ_t (10^{-16} cm^2)
0.04	69.4
0.1	61.7
0.4	48.9
1.0	42.3
2.0	38.1
5.0	33.6
10.	30.9
25.	27.8
Ref [71]	
37.5	32.1
50.	26.9
75.	23.1
100.	16.2
125.	6.81
150.	3.87
Ref [26]	

H–O^{8+}

E/M (keV/u)	σ_t (10^{-16} cm^2)
0.013	13.1
0.053	13.0
0.21	36.3
1.32	62.4
5.26	64.5
11.8	61.6
17.0	57.4
34.2	46.6
Ref [75]	
0.053	17.1
0.210	34.6
0.473	50.1
0.842	58.5
1.32	66.3
2.58	72.5
5.26	78.4
7.58	80.5
Ref [50]	
0.4	53.5
1.0	56.4
5.0	52.3
10.	48.2
25.	41.7
Ref [16]	
1.0	90.
2.0	86.
4.0	83.
8.	78.
10.	77.
20.	74.
Ref [45]	
17.8	51.1
39.1	43.1
57.1	37.1
75.6	28.0
97.5	19.5
121.	12.9
145.	8.36
168.	5.75
187.	4.25
Ref [22]	
37.5	36.7
50.	34.6
75.	28.5
100.	19.9
125.	11.7
150.	5.60
Ref [26]	
0.5	50.9
5.0	44.7
25.	35.4
50.	30.4
75.	27.4
100.	25.3
Ref [27]	

Table 4. Evaluated theoretical total charge exchange cross sections (σ_t) for the process $A^{Z+} + H \rightarrow A^{(Z-1)+} + H^+$ as a function of E/M, the laboratory energy of the ion divided by the mass of the ion (continued).

H-F^{9+}

E/M (keV/u)	σ_t (10^{-16}cm^2)
0.01	79.2
0.02	92.3
0.04	92.8
0.06	90.5
0.10	86.5
0.16	81.8
0.24	77.3
0.99	65.3
2.24	59.6
5.04	54.5
9.85	50.5
25.0	45.2
50.5	41.0
98.7	36.7
Ref [71]	
50.	37.6
Ref [65]	

H-Ne^{10+}

E/M (keV/u)	σ_t (10^{-16}cm^2)
0.04	66.8
0.06	73.2
0.09	78.5
0.16	83.6
0.20	84.9
0.25	85.4
0.50	85.0
1.0	81.8
4.0	70.3
6.2	65.9
8.9	62.8
16.1	57.1
24.8	53.0
50.1	47.2
Ref [71]	

E/M (keV/u)	σ_t (10^{-16}cm^2)
5.	53.9
10.	59.6
25.	58.0
50.	50.0
100.	28.5
200.	6.41
500.	.26
Ref [24]	
37.5	43.1
50.	41.1
75.	38.3
100.	27.5
150.	10.8
200.	3.51
Ref [26]	

H-Na^{11+}

E/M (keV/u)	σ_t (10^{-16}cm^2)
1.0	58.8
Ref [66]	
0.1	113.
1.0	88.5
10.	68.8
Ref [71]	
2.58	121.
Ref [7]	
1.0	120.
2.0	115.
4.0	110.
8.0	105.
10.	104.
20.	99.
40.	95.
Ref [45]	

H-Mg^{12+}

E/M (keV/u)	σ_t (10^{-16}cm^2)
0.5	145.
1.0	111.
Ref [66]	
0.1	116.
1.0	103.
10.	76.5
Ref [71]	
2.58	121.
Ref [7]	
1.0	130.
2.0	124.
4.0	118.
8.	113.
10.	112.
20.	105.
40.	100.
Ref [45]	
100.	35.7
Ref [65]	

H-Al^{13+}

E/M (keV/u)	σ_t (10^{-16}cm^2)
0.5	60.1
1.0	92.4
Ref [56]	
0.011	134.
0.014	137.
0.019	140.
0.026	142.
0.035	143.
0.046	143.
0.060	142.
0.078	139.
0.115	136.
0.155	133.
0.205	129.
0.245	127.
0.477	119.
0.981	111.
3.93	95.1
9.89	84.2
49.4	65.4
88.7	58.7
Ref [71]	
1.0	138.
2.0	133.
4.0	128.
8.0	123.
10.	122.
20.	116.
40.	111.
Ref [45]	

Table 4. Evaluated theoretical total charge exchange cross sections (σ_t) for the process $A^{Z+} + H \rightarrow A^{(Z-1)+} + H^+$ as a function of E/M, the laboratory energy of the ion divided by the mass of the ion (continued).

E/M (keV/u)	σ_t (10^{-16} cm^2)
H-Si^{14+}	
0.04	147.
0.09	148.
0.16	145.
0.25	140.
0.493	132.
0.997	121.
3.97	102.
8.98	92.4
10.1	90.3
16.1	83.9
25.1	79.1
50.4	69.7
Ref [71]	
5.	71.7
10.	68.2
25.	79.7
50.	79.6
100.	48.5
200.	14.6
500.	0.709
Ref [24]	
0.025	86.5
0.05	97.7
0.10	99.8
0.25	101.
0.50	94.
1.0	88.0
2.5	80.6
5.0	71.7
10.	65.8
25.	62.2
50.	59.3
100.	26.2
200.	5.0
500.	0.203
Ref [69]	

E/M (keV/u)	σ_t (10^{-16} cm^2)
37.5	62.1
50.	58.6
75.	53.7
100.	47.9
150.	19.6
200.	5.2
Ref [26]	
0.5	92.7
5.0	84.1
25.	69.7
50.	61.4
75.	56.2
100.	52.4
Ref [27]	
H-P^{15+}	
0.5	117.
1.0	144.
Ref [66]	
0.1	163.
1.0	136.
10.	100.
Ref [71]	
2.58	153.
Ref [7]	
1.0	159.
2.0	152.
4.0	146.
8.0	138.
10.	137.
20.	130.
40.	124.
Ref [45]	

E/M (keV/u)	σ_t (10^{-16} cm^2)
H-S^{16+}	
1.0	102.
Ref [66]	
0.1	177.
1.0	146.
10.	106.
Ref [71]	
2.58	159.
Ref [7]	
1.0	168.
2.0	161.
4.0	155.
8.0	148.
10.	147.
20.	140.
40.	134.
Ref [45]	
100.	56.9
Ref [65]	

E/M (keV/u)	σ_t (10^{-16} cm^2)
H-Cl^{17+}	
1.0	183.
Ref [66]	
0.04	204.
0.10	192.
0.40	170.
0.99	154.
4.0	130.
5.0	125.
10.	113.
25.	99.1
100.	77.6
Ref [71]	
2.58	165.
Ref [7]	
1.0	180.
2.0	172.
4.0	165.
8.0	157.
10.	156.
20.	148.
40.	141.
Ref [45]	

Table 4. Evaluated theoretical total charge exchange cross sections (σ_t) for the process $A^{Z+} + H \rightarrow A^{(Z-1)+} + H^+$ as a function of E/M, the laboratory energy of the ion divided by the mass of the ion (continued).

E/M (keV/u)	σ_t (10^{-16}cm^2)	E/M (keV/u)	σ_t (10^{-16}cm^2)	E/M (keV/u)	σ_t (10^{-16}cm^2)	E/M (keV/u)	σ_t (10^{-16}cm^2)
H-Ar^{18+}		**H-K^{19+}**		**H-Ca^{20+}**			
1.0	102.	1.0	195.	0.10	140.	0.04	253.
Ref [66]		Ref [66]		0.11	134.	0.10	237.
				0.13	129.	0.40	207.
0.04	220.	0.1	220.	0.15	123.	1.0	185.
0.10	209.	1.0	177.	0.18	118.	5.0	151.
0.40	183.	10.	129.	0.23	113.	10.	137.
0.60	177.	Ref [71]		0.29	110.	25.	117.
1.0	165.			0.36	108.	50.	104.
3.0	144.	2.58	177.	0.45	108.	100.	92.2
5.0	134.	Ref [7]		0.58	111.	Ref [71]	
10.	121.			0.71	114.		
25.	105.			0.85	118.	47.3	160.
50.	93.6	1.0	197.	1.1	123.	Ref [8]	
100.	81.8	2.0	189.	1.3	128.		
Ref [71]		4.0	182.	1.6	132.		
		8.0	174.	2.0	140.	1.0	208.
37.5	79.1	10.	173.	2.3	146.	2.0	200.
50.	80.1	20.	165.	2.7	151.	4.0	194.
75.	72.7	40.	158.	3.4	156.	8.0	188.
100.	60.8	Ref [45]		4.0	159.	10.	186.
150.	29.8			5.1	162.	20.	180.
200.	10.9			6.6	164.	40.	174.
Ref [26]		2.58	264.	8.2	165.	Ref [45]	
		47.3	196.	10.5	164.		
		Ref [9]		13.3	163.	100.	77.3
0.5	121.			16.3	162.	Ref [65]	
5.0	111.			19.9	159.		
25.	93.5			24.5	157.	0.1	137.
50.	83.2			30.1	154.	1.0	122.
75.	76.6			35.4	151.	10.	93.
100.	71.7			41.5	148.	Ref [24]	
Ref [27]				50.5	145.		
				60.6	141.		
				71.2	138.		
				Ref [66]			

Table 4. Evaluated theoretical total charge exchange cross sections (σ_t) for the process $A^{Z+} + H \rightarrow A^{(Z-1)+} + H^+$ as a function of E/M, the laboratory energy of the ion divided by the mass of the ion (continued).

E/M (keV/u)	σ_t (10^{-16} cm^2)	E/M (keV/u)	σ_t (10^{-16} cm^2)	E/M (keV/u)	σ_t (10^{-16} cm^2)	E/M (keV/u)	σ_t (10^{-16} cm^2)
H-Sc^{21+}		**H-Ti^{22+}**		**H-V^{23+}**		**H-Cr^{24+}**	
1.0	180.	1.0	194.	1.0	172.	1.0	221.
Ref [66]		Ref [66]		Ref [66]		Ref [66]	
0.15	247.	0.02	294.	0.1	277.0	0.04	317.
1.0	197.	0.04	285.	1.0	219.0	0.10	292.
10.	143.	0.06	275.	10.	158.0	0.20	274.
Ref [71]		0.10	265.	Ref [71]		0.40	254.
		0.16	253.			0.60	242.
2.58	189.	0.25	242.			1.0	228.
Ref [7]		0.50	225.	2.58	203.	2.0	210.
		1.0	207.	Ref [7]		5.0	183.
1.0	225.	2.22	187.			10.	166.
2.0	216.	5.0	167.			25.	143.
4.0	208.	10.0	152.	1.0	247.	50.	125.
8.0	200.	25.0	131.	2.0	238.	100.	110.
10.	198.	50.6	116.	4.0	230.	Ref [71]	
20.	190.	100.	103.	8.0	220.		
40.	182.	Ref [71]		10.	218.		
Ref [45]				20.	210.	2.58	209.
		2.58	196.	40.	202.	Ref [7]	
2.58	289.	Ref [7]		Ref [45]			
47.3	217.					1.0	256.
Ref [9]		1.0	238.	2.58	314.	2.0	246.
		2.0	228.	47.3	237.	4.0	236.
		4.0	220.	Ref [9]		8.0	228.
		8.0	212.			10.	225.
		10.	208.			20.	216.
		20.	200.			Ref [45]	
		40.	192.				
		Ref [45]					

Table 4. Evaluated theoretical total charge exchange cross sections (σ_t) for the process $A^{Z+} + H \rightarrow A^{(Z-1)+} + H^+$ as a function of E/M, the laboratory energy of the ion divided by the mass of the ion (continued).

E/M (keV/u)	σ_t (10^{-16} cm^2)
H-Mn^{25+}	
1.0	188.
Ref [66]	
0.1	305.
1.0	237.
10.	173.
Ref [71]	
2.58	215.
Ref [7]	
1.0	266.
2.0	256.
4.0	246.
8.0	237.
10.	234.
20.	224.
40.	214.
Ref [45]	
2.58	339.
47.3	258.
Ref [9]	

E/M (keV/u)	σ_t (10^{-16} cm^2)
H-Fe^{26+}	
0.21	201.
Ref [51]	
1.0	225.
Ref [66]	
0.02	362.
0.04	345.
0.10	319.
0.16	305.
0.25	291.
0.5	269.
1.0	248.
2.0	228.
5.0	201.
10.	181.
25.	154.
50.	133.
100.	122.
Ref [71]	
2.58	220.
Ref [7]	
1.0	276.
2.0	266.
4.0	256.
8.0	247.
10.	244.
Ref [45]	
0.5	176.
5.0	165.
25.	142.
50.	128.
75.	119.
100.	112.
Ref [27]	

E/M (keV/u)	σ_t (10^{-16} cm^2)
37.5	121.
50.	120.
75.	111.
100.	100.
150.	76.2
200.	28.6
Ref [26]	
H-Co^{27+}	
1.0	227.
Ref [66]	
0.1	335.
1.0	257.
10.	187.
Ref [71]	
2.58	226.
Ref [7]	
1.0	286.
2.0	276.
4.0	265.
8.0	255.
10.	254.
20.	240.
40.	230.
Ref [45]	
2.58	365.
47.3	278.
Ref [9]	

E/M (keV/u)	σ_t (10^{-16} cm^2)
H-Ni^{28+}	
1.0	222.
Ref [66]	
0.02	396.
0.04	379.
0.06	364.
0.10	349.
0.16	332.
0.25	317.
0.50	292.
1.0	269.
2.2	242.
5.0	218.
10.	196.
25.	169.
50.	150.
100.	131.
Ref [71]	
2.58	232.
Ref [7]	
1.0	296.
2.0	286.
4.0	275.
8.0	264.
10.	260.
Ref [45]	

Table 4. Evaluated theoretical total charge exchange cross sections (σ_t) for the process $A^{Z+} + H \rightarrow A^{(Z-1)+} + H^+$ as a function of E/M, the laboratory energy of the ion divided by the mass of the ion (continued).

E/M (keV/u)	σ_t (10^{-16} cm^2)
H-Cu^{29+}	
1.0	262.
Ref [66]	
0.04	394.
0.10	364.
0.40	315.
1.0	279.
2.2	255.
5.0	226.
10.	204.
25.	174.
100.	132.
Ref [71]	
2.58	238.
Ref [7]	
1.0	305.
2.0	295.
4.0	285.
8.0	274.
10.	270.
20.	260.
Ref [45]	

E/M (keV/u)	σ_t (10^{-16} cm^2)
H-Zn^{30+}	
0.08	290.
0.10	283.
0.12	277.
0.14	269.
0.16	261.
0.20	251.
0.23	243.
0.31	235.
0.40	232.
0.54	231.
0.70	235.
0.86	239.
1.1	244.
1.4	248.
1.8	250.
2.2	250.
2.9	251.
3.9	248.
5.5	243.
8.2	237.
13.2	232.
20.6	227.
32.1	221.
Ref [66]	

E/M (keV/u)	σ_t (10^{-16} cm^2)
0.1	375.
1.0	288.
10.	209.
Ref [71]	
2.58	244.
Ref [7]	
47.3	250.
Ref [8]	
1.0	316.
2.0	306.
4.0	296.
8.0	284.
10.	280.
20.	270.
40.	258.
80.	248.
100.	244.
Ref [45]	
H-Ga^{31+}	
0.1	389.
1.0	298.
10.	217.
Ref [71]	
2.58	250.
Ref [7]	

E/M (keV/u)	σ_t (10^{-16} cm^2)
H-Ge^{32+}	
0.1	405.
1.0	309.
10.	224.
Ref [71]	
2.58	255.
Ref [7]	
H-As^{33+}	
0.1	416.
1.0	317.
10.	229.
Ref [71]	
2.58	260.
Ref [7]	
H-Se^{34+}	
0.1	430.
1.0	329.
10.	237.
Ref [71]	
2.58	265.
Ref [7]	

Table 4. Evaluated theoretical total charge exchange cross sections (σ_t) for the process $A^{Z+} + H \rightarrow A^{(Z-1)+} + H^+$ as a function of E/M, the laboratory energy of the ion divided by the mass of the ion (continued).

E/M (keV/u)	σ_t (10^{-16} cm^2)
H-Br^{35+}	
0.1	444.
1.0	338.
10.	243.
Ref [71]	
2.58	271.
Ref [7]	
H-Kr^{36+}	
0.02	532.
0.04	504.
0.09	465.
0.16	438.
0.25	418.
0.40	394.
1.0	353.
2.0	324.
5.0	285.
10.	254.
25.	216.
100.	169.
Ref [71]	
2.58	276.
Ref [7]	
37.5	166.
50.0	158.
75.0	153.
100.	141.
150.	106.
200.	60.
Ref [26]	

E/M (keV/u)	σ_t (10^{-16} cm^2)
0.5	246.
5.0	232.
25.	205.
50.0	187.
75.0	175.
100.	165.
Ref [27]	
H-Rb^{37+}	
0.1	472.
1.0	357.
10.	258.
Ref [71]	
2.58	281.
Ref [7]	
H-Sr^{38+}	
0.1	486.
1.0	368.
10.	266.
Ref [71]	
2.58	287.
Ref [7]	

E/M (keV/u)	σ_t (10^{-16} cm^2)
H-Y^{39+}	
0.1	500.
1.0	379.
10.	274.
Ref [71]	
2.58	292.
Ref [7]	
H-Zr^{40+}	
0.02	599.
0.04	568.
0.10	516.
0.20	478.
0.4	442.
1.0	393.
2.8	344.
5.0	316.
10.	283.
25.	243.
50.	212.
100.	187.
Ref [71]	
2.58	296.
Ref [7]	
H-Cb^{41+}	
0.1	529.
1.0	400.
10.	287.
Ref [71]	
2.58	303.
Ref [7]	

E/M (keV/u)	σ_t (10^{-16} cm^2)
H-Mo^{42+}	
0.04	598.
0.10	544.
0.20	503.
0.40	465.
1.0	413.
3.0	361.
5.0	333.
10.0	297.
25.	255.
100.	195.
Ref [71]	
2.58	309.
Ref [7]	
H-Tc^{43+}	
0.1	557.
1.0	420.
10.	303.
Ref [71]	
2.58	315.
Ref [7]	
H-Ru^{44+}	
0.1	572.
1.0	431.
10.	311.
Ref [71]	
2.58	320.
Ref [7]	

Table 4. Evaluated theoretical total charge exchange cross sections (σ_t) for the process $A^{Z+} + H \rightarrow A^{(Z-1)+} + H^+$ as a function of E/M, the laboratory energy of the ion divided by the mass of the ion (continued).

H-Rb^{45+}

E/M (keV/u)	σ_t (10^{-16} cm^2)
0.1	586.
1.0	442.
10.	319.
Ref [71]	
2.58	327.
Ref [7]	

H-Pd^{46+}

E/M (keV/u)	σ_t (10^{-16} cm^2)
0.1	598.
1.0	452.
10.	327.
Ref [71]	
2.58	334.
Ref [7]	

H-Ag^{47+}

E/M (keV/u)	σ_t (10^{-16} cm^2)
0.1	612.
1.0	462.
10.	334.
Ref [71]	
2.58	340.
Ref [7]	

H-Cd^{48+}

E/M (keV/u)	σ_t (10^{-16} cm^2)
0.02	718.
0.04	677.
0.10	624.
0.20	584.
0.40	538.
1.0	477.
2.0	430.
5.0	383.
10.	345.
25.	294.
100.	227.
Ref [71]	
2.58	346.
Ref [7]	

H-In^{49+}

E/M (keV/u)	σ_t (10^{-16} cm^2)
0.1	641.
1.0	480.
10.	347.
Ref [71]	
2.58	353.
Ref [7]	

H-Sn^{50+}

E/M (keV/u)	σ_t (10^{-16} cm^2)
0.1	655.
1.0	491.
10.	355.
Ref [71]	
2.58	359.
Ref [7]	

H-Sb^{51+}

E/M (keV/u)	σ_t (10^{-16} cm^2)
0.1	668.
1.0	502.
10.	362.
Ref [71]	

H-Te^{52+}

E/M (keV/u)	σ_t (10^{-16} cm^2)
0.1	682.
1.0	512.
10.	370.
Ref [71]	

H-I^{53+}

E/M (keV/u)	σ_t (10^{-16} cm^2)
0.1	696.
1.0	523.
10.	378.
Ref [71]	

H-Xe^{54+}

E/M (keV/u)	σ_t (10^{-16} cm^2)
0.02	833.
0.04	779.
0.10	710.
0.4	607.
1.0	539.
5.0	432.
10.	384.
25.	332.
100.	254.
Ref [71]	

H-W^{74+}

E/M (keV/u)	σ_t (10^{-16} cm^2)
0.21	900.
0.35	847.
1.0	745.
2.0	678.
5.0	600.
10.	538.
25.	452.
100.	345.
Ref [71]	

Table 5. Partial cross sections (σ_n) for the process $H + A^{Z+} \rightarrow H^+(n) + A^{(Z-1)+}$ given in units of 10^{-16} cm^2.

E/M (keV/u) \ n	1	2	3	4	5	6	7	8	9	10	11	12	13	14
H-Li^{3+}														
1.0	0.34	1.20	2.34											
5.0	0.066	5.15	5.06											
10	0.00	6.61	9.37											
25	0.001	6.05	7.18											
100	0.005	0.563	0.557											
200	0.007	0.063	0.054											
					Ref [67]									
50	0.009	2.62	4.34	3.27										
100	0.017	0.581	0.715	0.410										
200	0.010	0.069	0.580	0.033										
					Ref [72]									
50		2.76	2.70	1.24	0.590	0.328	0.202	0.118						
					Ref [65]									
14	0.041	16.9	10.4											
29	0.028	6.37	6.27											
43	0.024	3.10	3.34											
57	0.022	1.72	1.80											
71	0.021	1.03	1.03											
86	0.019	0.65	0.614											
100	0.017	0.430	0.383											
114	0.016	0.293	0.248											
143	0.013	0.148	0.114											
179	0.010	0.071	0.049											
214	0.0076	0.0368	0.0236											
285	0.0044	0.0123	0.0061											
					Ref [64]									
132	0.017	0.178	0.150	0.094	0.058	0.038	0.026	0.018	0.013	0.010	0.008	0.006		
					Ref [58]									

Table 5. Partial cross sections (σ_n) for the process $H + A^{Z+} \rightarrow H^+(n) + A^{(Z-1)+}$ given in units of 10^{-16} cm^2 (continued).

E/M (keV/u) \ n	1	2	3	4	5	6	7	8	9	10	11	12	13	14
H-Be^{4+}														
5		5.89	43.4	0.38	0.05									
10		6.99	31.6	3.16	0.22									
25		4.42	14.2	6.49	2.17									
50		1.96	5.06	3.53	1.96									
100		0.597	1.09	0.879	0.584									
200		0.112	0.138	0.104	0.069									
					Ref [17]									
50		1.48	4.56	3.28	1.68	0.804	0.462	0.272	0.229	0.157				
100		0.436	0.790	0.706	0.460	0.321	0.207	0.148	0.102					
					Ref [65]									
132		0.189	0.309	0.253	0.179	0.125	0.089	0.064	0.048	0.036	0.028	0.022	0.018	0.015
	0.003				Ref. [58]									
H-B^{5+}														
0.5			6.33	2.94										
1.0			8.40	2.07										
10			11.8	0.668										
25			12.2	0.421										
					Ref [16]									
5.0		2.10	49.6	13.0	0.14									
10		2.16	37.2	18.5	1.37									
25		1.75	16.5	14.4	5.59									
50		1.03	6.14	6.23	3.91									
100		0.41	1.45	1.51	1.11									
					Ref [17]									
25		0.518	10.3	10.3	0.855	0.473								
32		0.329	8.41	9.96	1.58	0.88	0.31							
					Ref [49]									

Table 5. Partial cross sections (σ_n) for the process $H + A^{Z+} \rightarrow H^+(n) + A^{(Z-1)+}$ given in units of 10^{-16} cm^2 (continued).

n / E/M (keV/u)	1	2	3	4	5	6	7	8	9	10	11	12	13	14	15
H-Be^{5+}															
50		0.397	4.92	6.13	3.26	1.65	1.11	0.512	0.322	0.214					
					Ref [65]										
73		0.262	2.71	3.43	3.91	1.66	0.924	0.639	0.477						
					Ref [49]										
132	0.002	0.123	0.409	0.461	0.383	0.292	0.219	0.165	0.126	0.098	0.077	0.062	.050	.041	.034
					Ref [58]										
H-C^{6+}															
0.013				0.470											
0.053				3.82	0.390										
0.135				11.0	3.28										
0.21				16.2	4.80										
0.64				29.9	6.45										
1.32				37.4	6.62										
2.96				38.1	7.76										
5.26			1.07	36.6	9.47										
11.8			2.13	29.0	12.5										
21.0			2.24	23.4	12.2										
27.4			1.96	20.3	12.3										
					Ref [10]										
0.50			0.022	35.9											
1.0			0.131	39.1											
10			2.17	33.3											
25			3.40	27.3											
					Ref [16]										
25		0.07	5.49	16.8	3.76	0.842	0.376	0.141	0.087	0.050	0.019				
50		0.14	2.91	7.10	6.01	3.06	1.36	0.747	0.492	0.315	0.233	0.138	0.095	0.092	
75		0.125	1.64	3.28	2.97	2.19	1.50	1.03	0.700	0.475	0.402	0.286	0.232	0.184	
100		0.116	0.851	1.43	1.51	1.19	0.903	0.647	0.467	0.352	0.290	0.225	0.192	0.166	
					Ref [65]										

Table 5. Partial cross sections (σ_n) for the process $H + A^{Z+} \rightarrow H^+(n) + A^{(Z-1)+}$ given in units of 10^{-16} cm^2 (continued).

E/M (keV/u) \ n	1	2	3	4	5	6	7	8	9	10	11	12	13	14
H-C^{6+}														
132	0.001	0.061	0.398	0.639	0.639	0.542	0.433	0.341	0.268	0.213	0.171	0.138	0.113	0.094
					Ref [58]									
200		0.0057	0.088	0.168	0.181	0.169	0.134	0.110	0.090	0.071	0.056	0.045	0.037	0.030
					Ref [62]									
H-N^{7+}														
0.5				15.6	31.6									
1.0				18.3	24.0									
10				22.0	8.84									
25			0.131	21.9	5.76									
					Ref [16]									
50			1.41	6.89	7.55	5.24	2.51	1.15	0.740	0.413	0.285			
					Ref [65]									
H-O^{8+}														
0.0132					0.80	12.3								
0.0526					5.42	7.52	0.02							
0.210					21.8	14.3	0.09							
1.32				0.26	47.2	15.0	0.18							
5.26				3.78	45.0	17.8	0.39							
11.8				5.31	36.1	20.2	1.34							
17.0				4.80	31.6	20.3	2.23							
34.2				2.88	21.5	22.9	2.66							
					Ref [75]									
0.5				1.54	51.1	1.98								
1.0				3.18	51.8	1.41								
10				9.57	38.2	0.45								
25				11.3	30.1	0.29								
					Ref [16]									

Table 5. Partial cross sections (σ_n) for the process $H + A^{Z+} \rightarrow H^+(n) + A^{(Z-1)+}$ given in units of 10^{-16} cm^2 (continued).

E/M (keV/u) \ n	1	2	3	4	5	6	7	8	9	10	11	12	13	14
H-O^{8+}														
50			0.548	5.09	10.0	7.89	4.33	1.95	0.990	0.604	0.321	0.665	0.421	0.350
100			0.387	1.35	2.41	2.31	1.96	1.58	1.18	0.908	0.724			
					Ref [65]									
200			0.032	0.147	0.300	0.351	0.332	0.308	0.267	0.222	0.186	0.158	0.132	0.115
					Ref [62]									
H-F^{9+}														
0.5					26.2	48.8	0.047							
1.0				0.064	29.8	38.2	0.034							
10				2.24	32.8	15.1	0.01							
25				4.04	30.7	10.0	0.01							
					Ref [16]									
50			0.213	0.321	10.4	10.4	6.75	2.88	1.34	0.873	0.562			
					Ref [65]									
H-Ne^{10+}														
0.5					5.56	66.0	8.79							
1.0					9.05	63.1	6.30							
10				0.036	18.9	40.1	2.09							
25				1.17	20.4	30.3	1.33							
					Ref [16]									
1.0		0.052	0.421	4.11	12.8	52.0	8.67	0.815	1.92	2.74				
5.0			0.153	0.889	14.3	42.2	12.3	5.57	4.21	1.69				
10			0.194	1.93	15.9	29.3	8.23	6.32	2.14	0.354				
25			0.836	3.59	12.7	18.8	2.96	2.55	0.435	0.0111				
50			0.801	2.99	6.88	9.02	0.625	0.527	0.0143					
100		0.008	0.464	1.51	2.66	3.21	0.0216	0.0177						
200		0.010	0.201	0.472	0.654	0.692								
500		0.0012	0.0233	0.0314	0.0316	0.0276								
					Ref [24]									

Table 5. Partial cross sections (σ_n) for the process $H + A^{Z+} \rightarrow H^+(n) + A^{(Z-1)+}$ given in units of 10^{-16} cm^2 (continued).

E/M (keV/u) \ n	1	2	3	4	5	6	7	8	9	10	11	12	13	14
H-Ne^{10+}														
50				1.51	7.50	11.6	10.2	4.94	2.27	1.11	0.670	0.379	0.289	0.758
100				0.801	1.99	2.87	3.07	2.68	2.42	1.85	1.54	1.25	0.965	
					Ref [65]									
H-Na^{11+}														
0.5					0.26	40.0	56.0	0.79						
1.0					0.96	43.9	43.9	0.57						
					Ref [16]									
H-Mg^{12+}														
0.5						14.0	77.4	15.6	0.04					
1.0					0.04	19.4	70.3	11.3	0.03					
10.0					2.46	30.1	39.4	3.86						
25.0				0.10	4.83	29.8	38.8	2.49						
					Ref [16]									

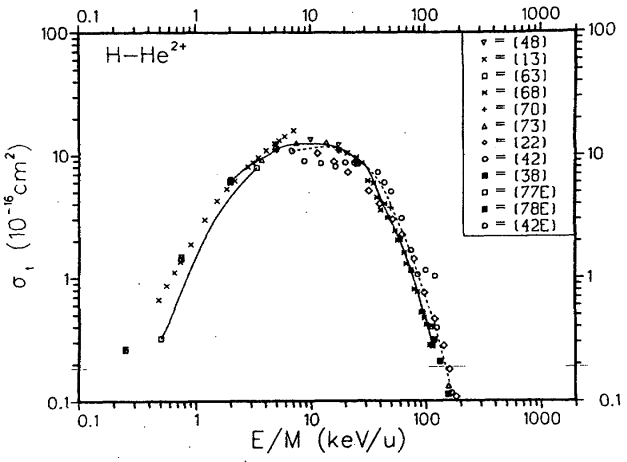

FIGURE 1. Evaluated total charge exchange cross sections for $H + He^{2+} \rightarrow H^+ + He^+$ as functions of E/M.

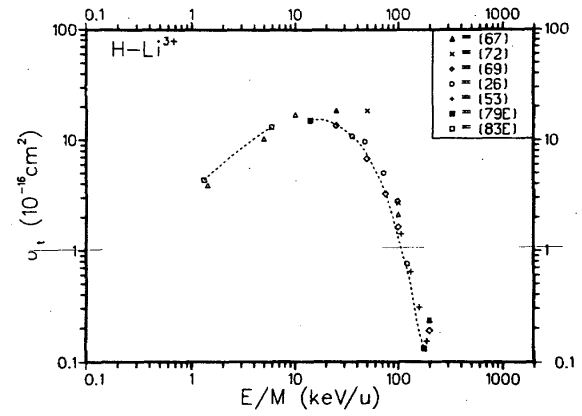

FIGURE 2. Evaluated total charge exchange cross sections for $H + Li^{3+} \rightarrow H^+ + Li^{2+}$.

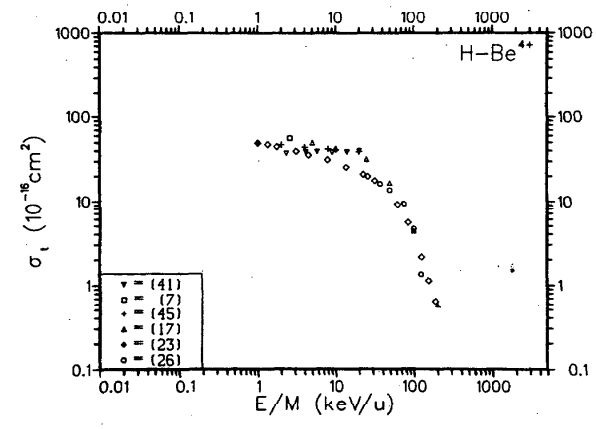

FIGURE 3. Evaluated total charge exchange cross sections for $H + Be^{4+} \rightarrow H^+ + Be^{3+}$.

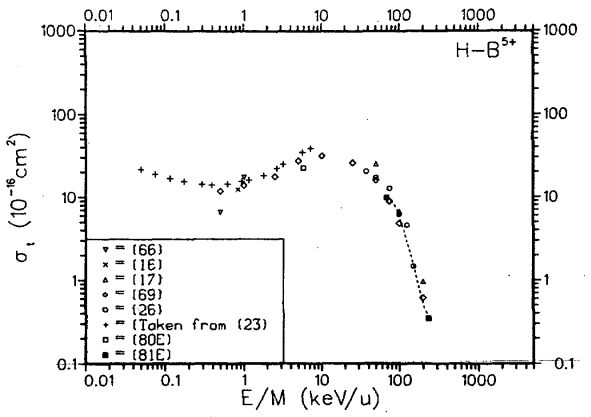

FIGURE 4. Evaluated total charge exchange cross sections for $H + B^{5+} \rightarrow H^+ + B^{4+}$.

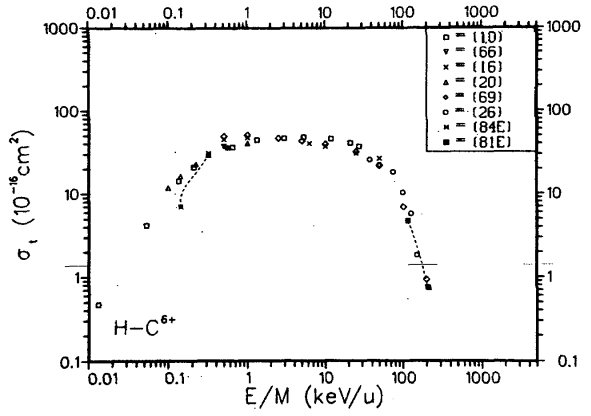

FIGURE 5. Evaluated total charge exchange cross sections for $H + C^{6+} \rightarrow H^+ + C^{5+}$.

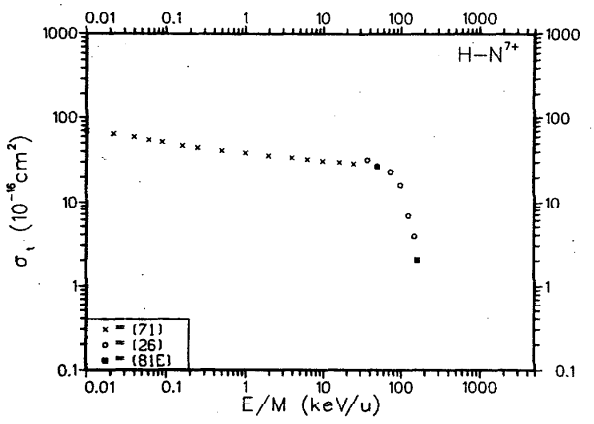

FIGURE 6. Evaluated total charge exchange cross sections for $H + N^{7+} \rightarrow H^+ + N^{6+}$.

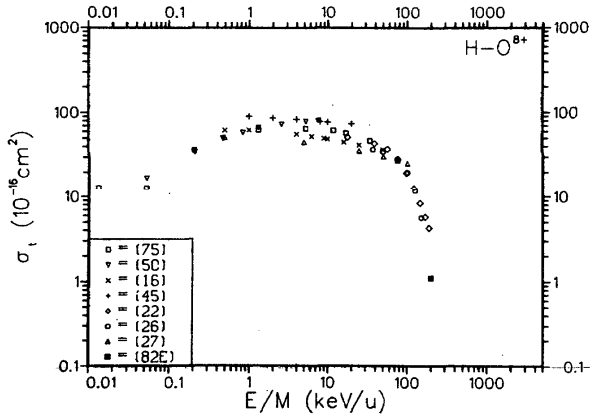

FIGURE 7. Evaluated total charge exchange cross sections for $H + O^{8+} \rightarrow H^+ + O^{7+}$.

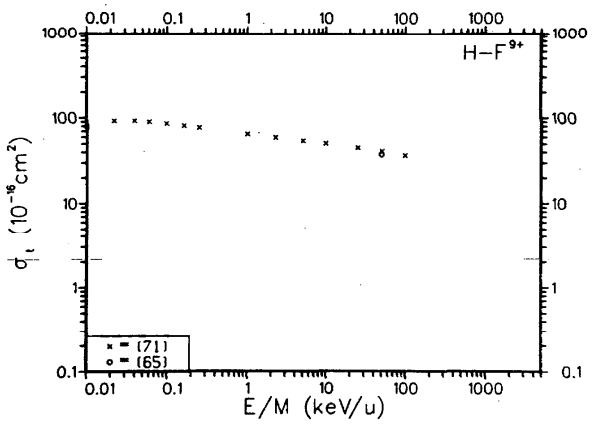

FIGURE 8. Evaluated total charge exchange cross sections for $H + F^{9+} \rightarrow H^+ + F^{8+}$.

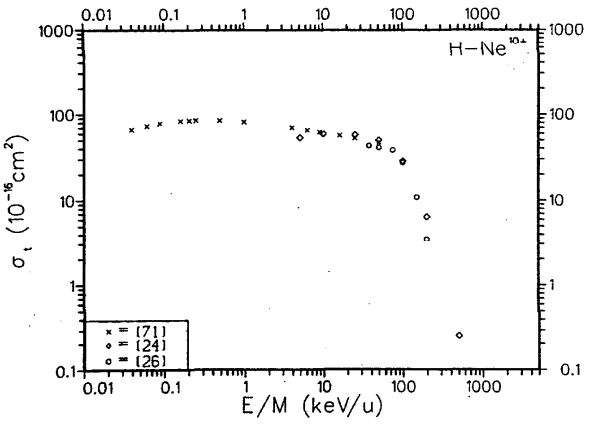

FIGURE 9. Evaluated total charge exchange cross sections for $H + Ne^{10+} \rightarrow H^+ + Ne^{9+}$.

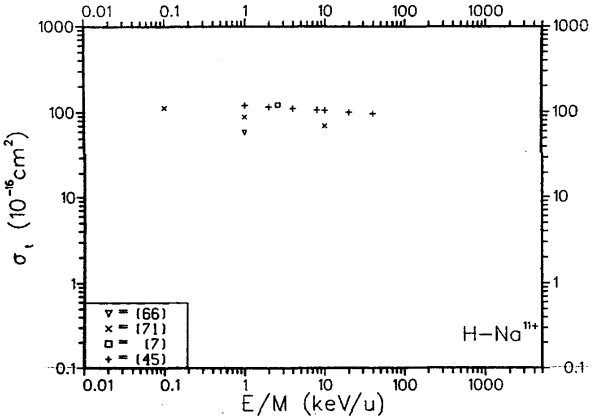

FIGURE 10. Evaluated total charge exchange cross sections for $H + Na^{11+} \rightarrow H^+ + Na^{10+}$.

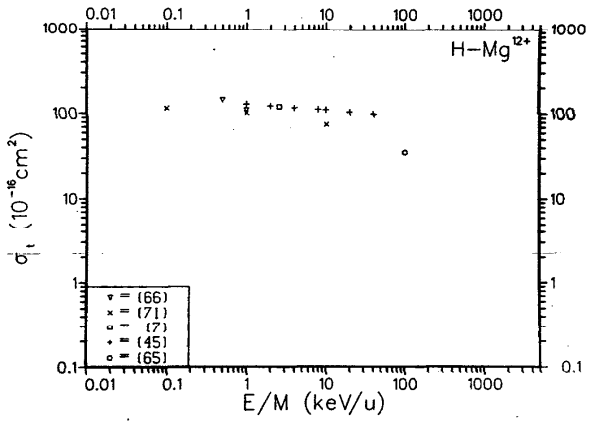

FIGURE 11. Evaluated total charge exchange cross sections for $H + Mg^{12+} \rightarrow H^+ + Mg^{11+}$.

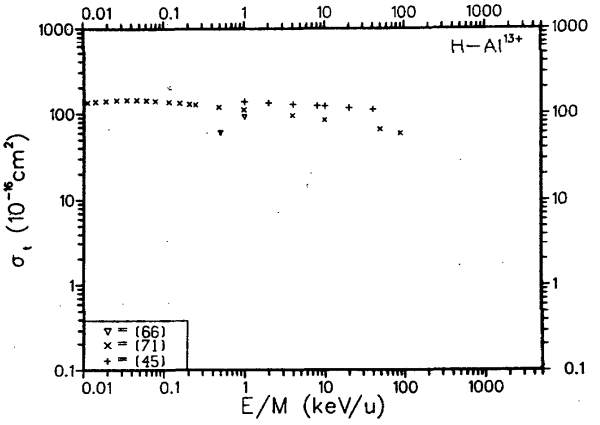

FIGURE 12. Evaluated total charge exchange cross sections for $H + Al^{13+} \rightarrow H^+ + Al^{12+}$.

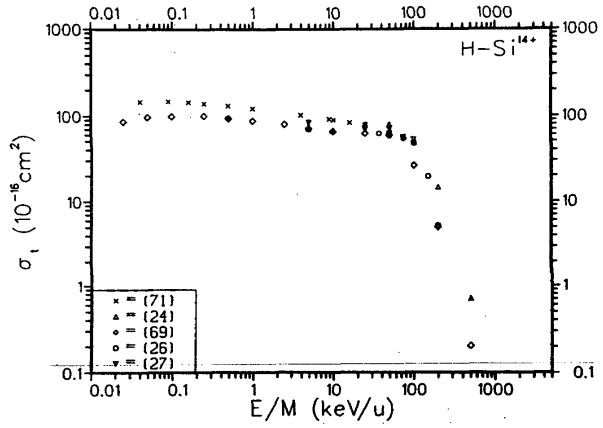

FIGURE 13. Evaluated total charge exchange cross sections for $H + Si^{14+} \rightarrow H^+ + Si^{13+}$

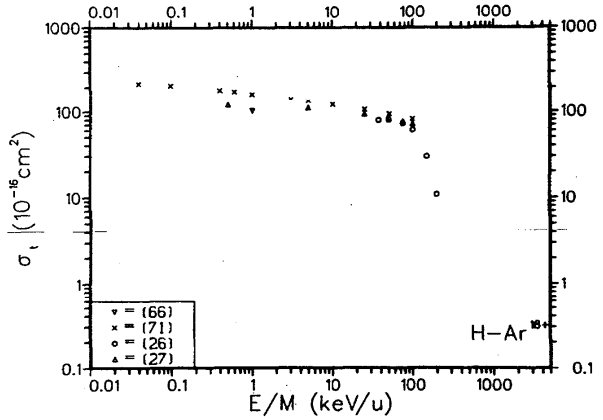

FIGURE 14. Evaluated total charge exchange cross sections for $H + Ar^{18+} \rightarrow H^+ + Ar^{17+}$.

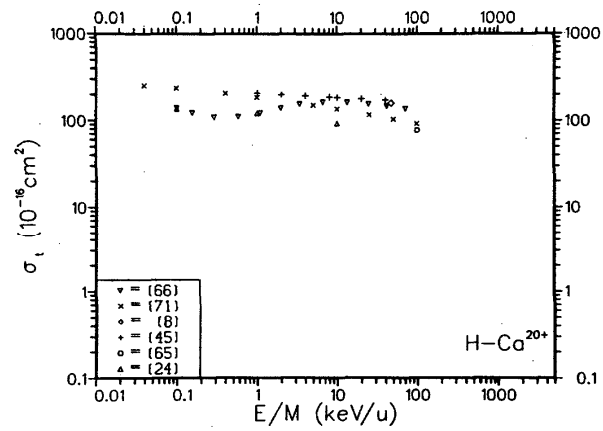

FIGURE 15. Evaluated total charge exchange cross sections for $H + Ca^{20+} \rightarrow H^+ + Ca^{19+}$.

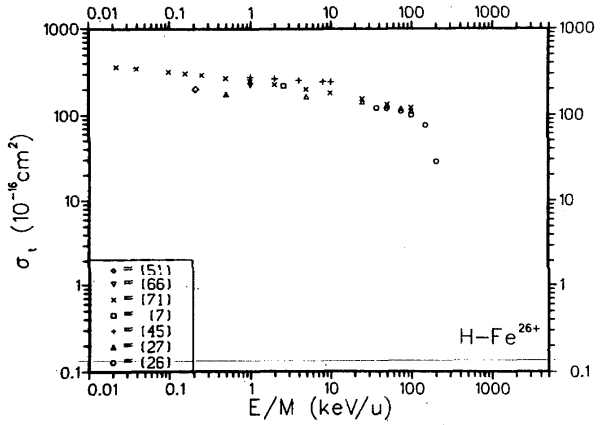

FIGURE 16. Evaluated total charge exchange cross sections for $H + Fe^{26+} \rightarrow H^+ + Fe^{25+}$.

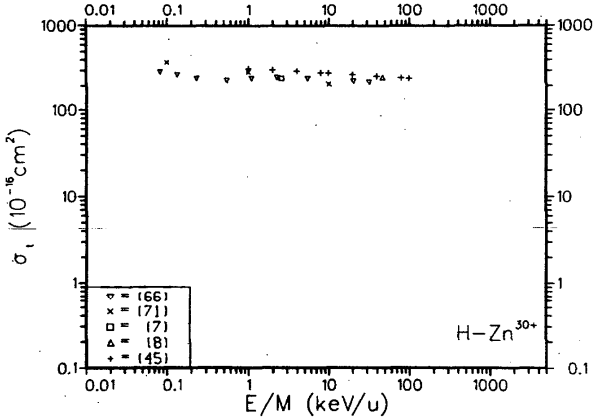

FIGURE 17. Evaluated total charge exchange cross sections for $H + Zn^{30+} \rightarrow H^+ + Zn^{29+}$.

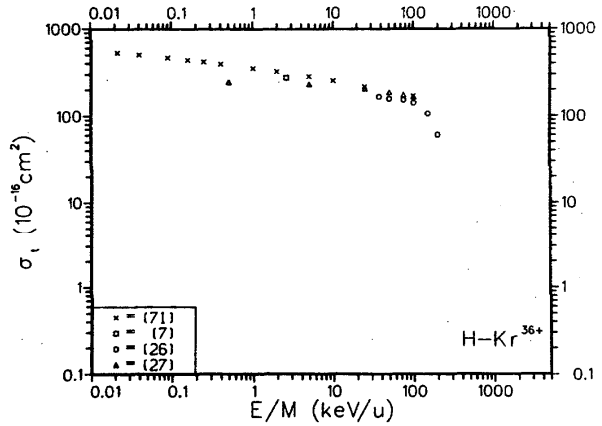

FIGURE 18. Evaluated total charge exchange cross sections for $H + Kr^{36+} \rightarrow H^+ + Kr^{35+}$.

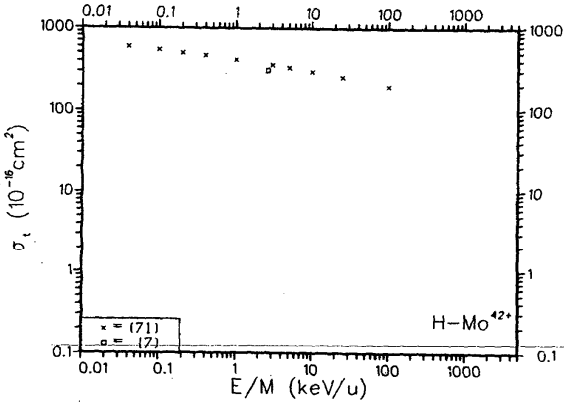

FIGURE 19. Total charge exchange cross section for $H + Mo^{42+} \rightarrow H^+ + Mo^{41+}$.

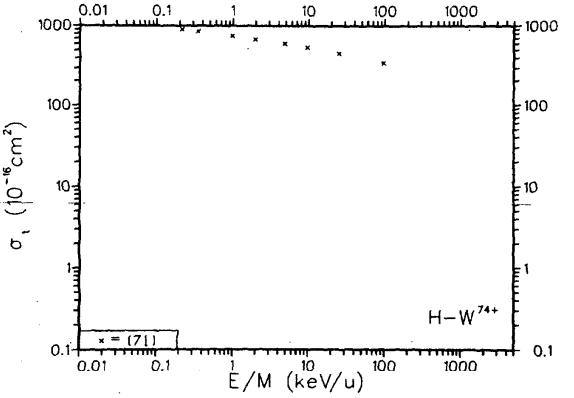

FIGURE 20. Total charge exchange cross section for $H + W^{74+} \rightarrow H^+ + W^{73+}$.

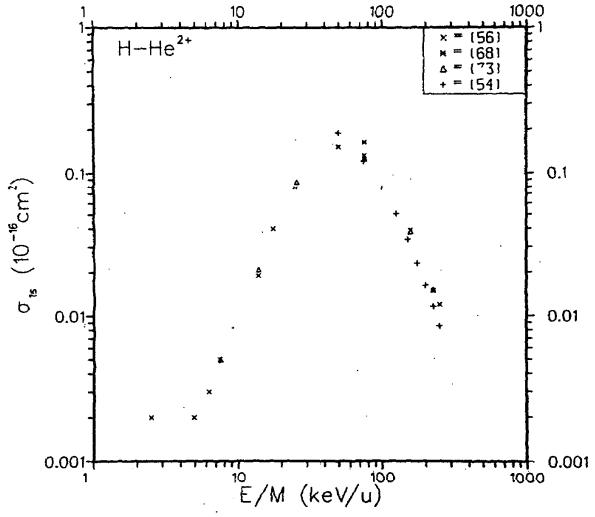

FIGURE 21. Evaluated partial charge exchange cross sections for $H(1s) + He^{2+} \rightarrow H^+ + He^+(1s)$.

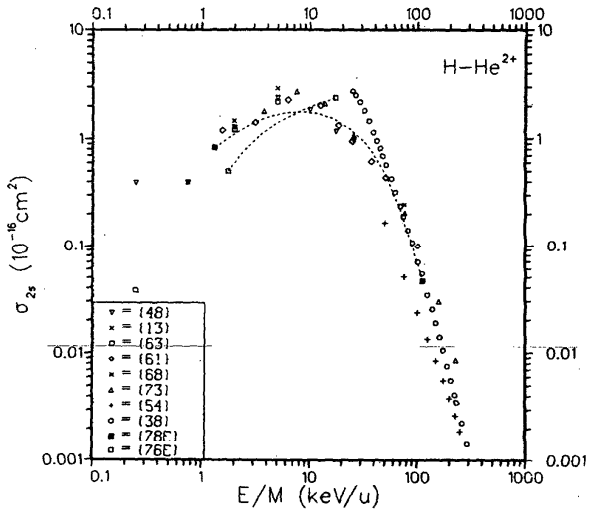

FIGURE 22. Evaluated partial charge exchange cross sections for $H(1s) + He^{2+} \rightarrow H^+ + He^+(2s)$.

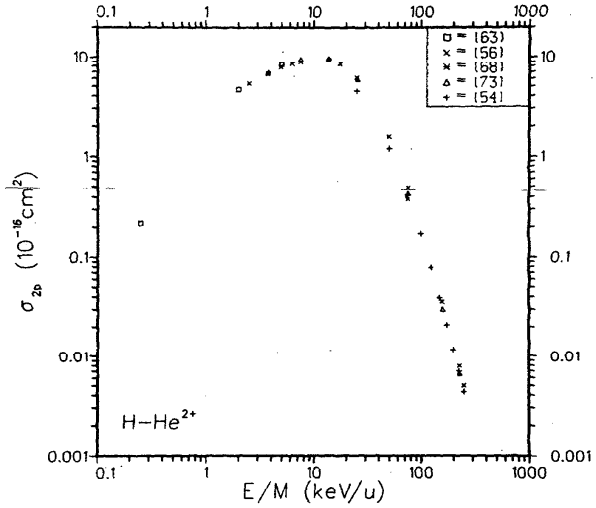

FIGURE 23. Evaluated partial charge exchange cross sections for $H(1s) \rightarrow He^{2+} \rightarrow H^+ + He^+(2p)$.

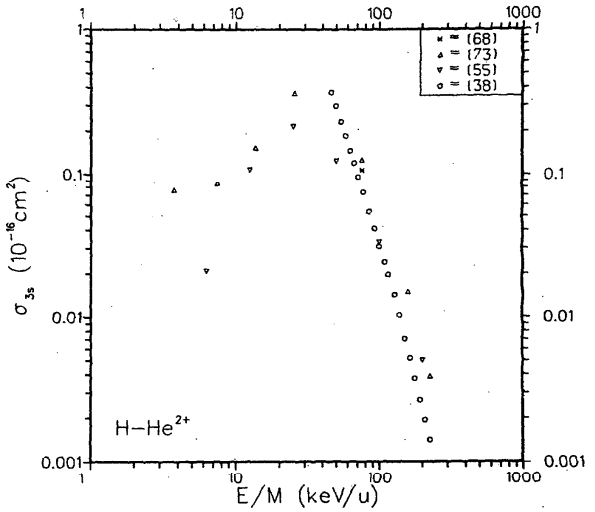

FIGURE 24. Evaluated partial charge exchange cross sections for $H(1s) + He^{2+} \rightarrow H^+ + He^+(3s)$.

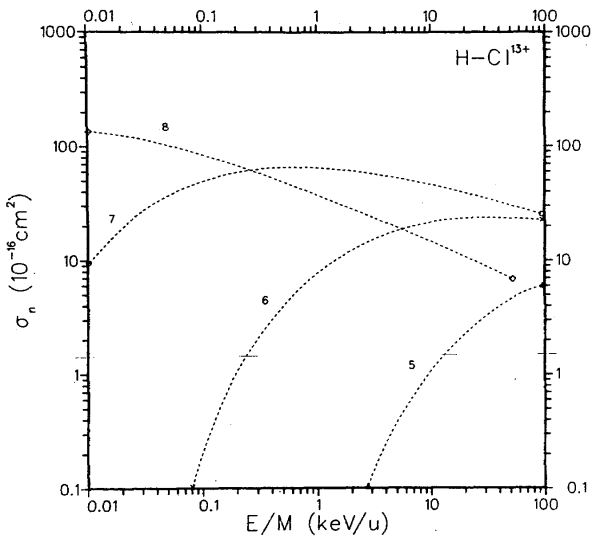

FIGURE 25. Partial charge exchange cross sections for $H + Cl^{13+} \rightarrow H^+ + Cl^{12+}(n)$. The numbers in the figure give the values of n. Data are from Ref. 71.

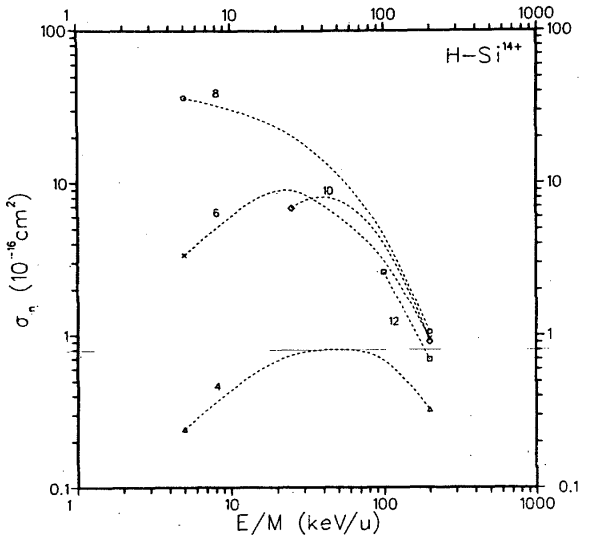

FIGURE 27. Partial charge exchange cross sections for $H + Si^{14+} \rightarrow H^+ + Si^{13(+)}(n)$. The numbers in the figure give the values of n. Data are from Ref. 24.

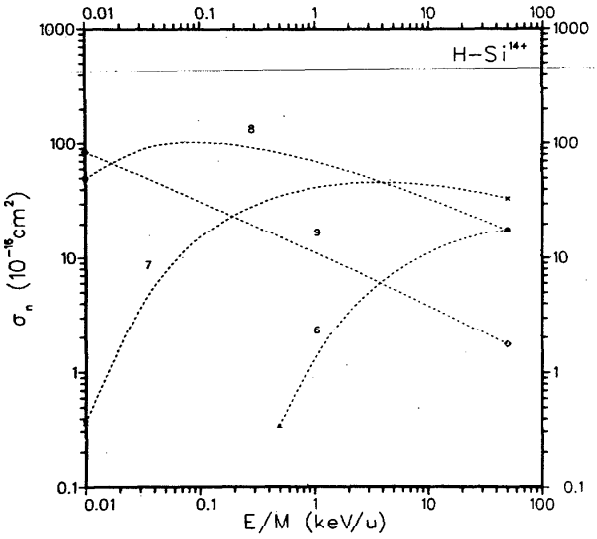

FIGURE 26. Partial charge exchange cross sections for $H + Si^{14+} \rightarrow H^+ + Si^{13+}(n)$. The numbers in the figure give the values of n. Data are from Ref. 71.

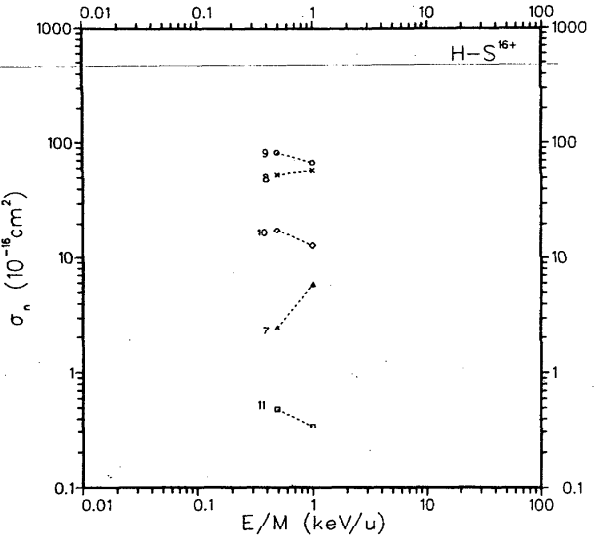

FIGURE 28. Partial charge exchange cross sections for $H + S^{16+} \rightarrow H^+ + S^{15+}(n)$. The numbers in the figure give the values of n. Data are from Ref. 71.

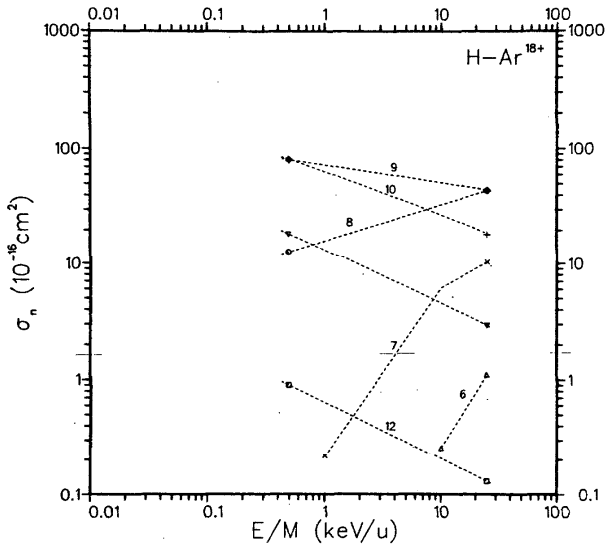

FIGURE 29. Partial charge exchange cross sections for $H + Ar^{18+} \rightarrow H^+ + Ar^{17(+)}(n)$. The numbers in the figure give the values of n. Data are from Ref. 71.

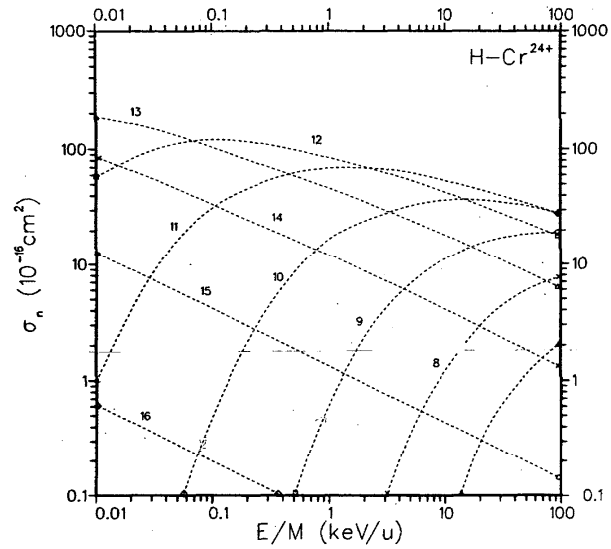

FIGURE 31. Partial charge exchange cross sections for $H + Cr^{24+} \rightarrow H^+ + Cr^{23+}(n)$. The numbers in the figure give the values of n. Data are from Ref. 71.

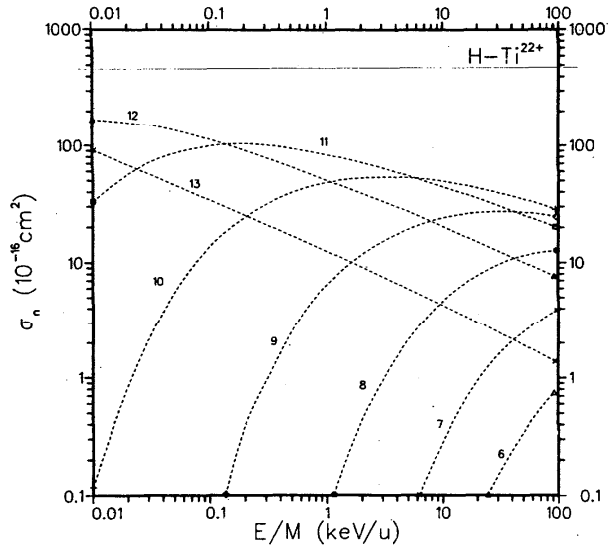

FIGURE 30. Partial charge exchange cross sections for $H + Ti^{22+} \rightarrow H^+ + Ti^{21(+)}(n)$. The numbers in the figure give the values of n. Data are from Ref. 71.

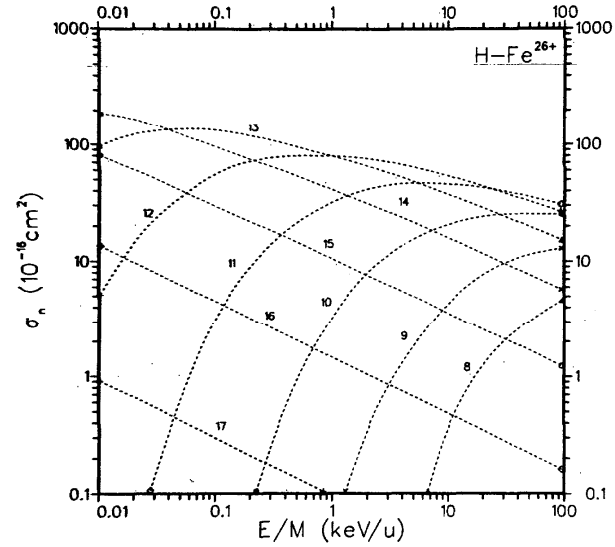

FIGURE 32. Partial charge exchange cross sections for $H + Fe^{26+} \rightarrow H^+ + Fe^{25+}(n)$. The numbers in the figure give the values of n. Data are from Ref. 71.

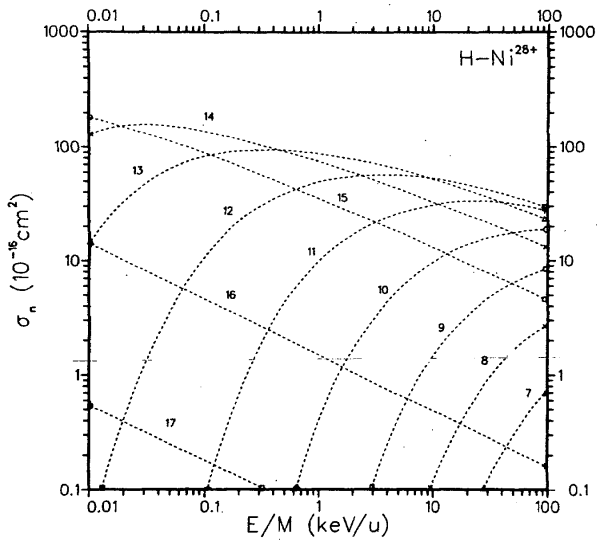

FIGURE 33. Partial charge exchange cross sections for $H + Ni^{28+} \rightarrow H^+ + Ni^{27+}(n)$. The numbers in the figure give the values of n. Data are from Ref. 71.

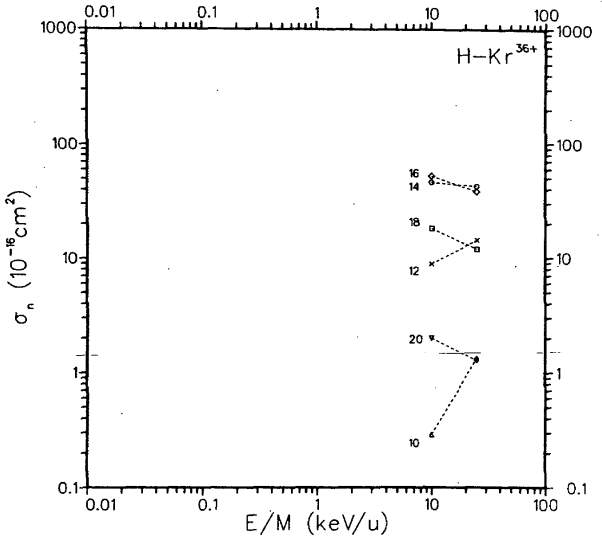

FIGURE 34. Partial charge exchange cross sections for $H + Kr^{36+} \rightarrow H^+ + Kr^{35+}(n)$. The numbers in the figure give the values of n. Data are from Ref. 71.

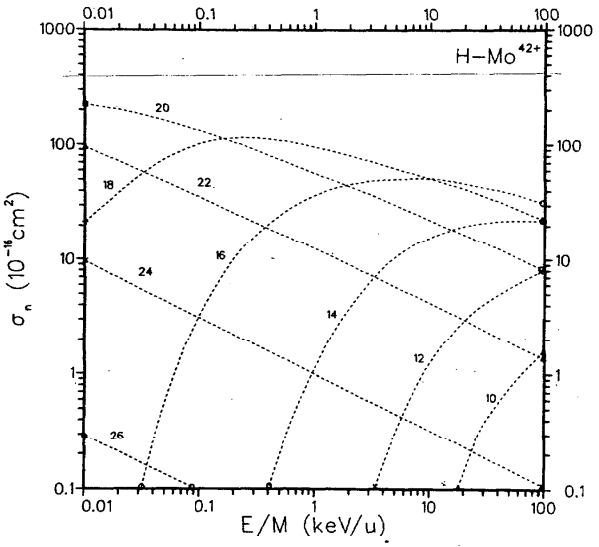

FIGURE 35. Partial charge exchange cross sections for $H + Mo^{42+} \rightarrow H^+ + Mo^{41+}(n)$. The numbers in the figure give the values of n. Data are from Ref. 71.

6. Acknowledgments

R.K.J. and B.H.B. would like to express their gratitude to the JILA staff for the hospitality extended to them during their Visiting Fellowships. The partial support to this work by the National Bureau of Standards, the Office of Fusion Energy, U.S. Department of Energy and the International Atomic Energy Agency, Vienna, Austria (Contract No. 2857/R1/RB with R.K.J.) is gratefully acknowledged.

7. References

[1]R. E. Olson, in *The Physics of Electronic and Atomic Collisions*, edited by N. Oda and K. Takayanagi (North–Holland, Amsterdam, 1980), p. 391.
[2]E. Salzborn, in *Atomic Processes in Fusion Plasmas*, edited by Y. Itikawa and T. Kato (IPPJ-AM-13, 1979), p. 44.
[3]H. B. Gilbody, Physica Scripta **23** (No. 2), 143 (1981).
[4]R. K. Janev and L. P. Presnyakov, Phys. Rep. **70**, 1 (1981).
[5]N. F. Mott and H. S. W. Massey, *The Theory of Atomic Collisions*, 3rd ed. (Oxford University, Oxford, 1971).
[6]A. Salop and R. E. Olson, Phys. Rev. A **13**, 1312 (1976).
[7]R. E. Olson and A. Salop, Phys. Rev. A **14**, 579 (1976).
[8]M. I. Chibisov [Pisma Zh. Eksp. Teor. Fiz. **24**, 56 (1976)] JETP Lett. **24**, 46 (1976).
[9]T. P. Grozdanov and R. K. Janev, Phys. Rev. A **17**, 880 (1978).
[10]T. A. Green, E. J. Shipsey, and J. C. Browne, Phys. Rev. A **25**, 1364 (1982).
[11]D. R. Bates and R. McCarroll, Proc. R. Soc. (London) Ser. A **245**, 175 (1958).
[12]R. D. Piacentini and A. Salin, J. Phys. B **7**, 1666 (1974).
[13]D. S. F. Crothers and N. R. Todd, J. Phys. B **14**, 3251 (1981).
[14]L. P. Presnyakov, D. B. Uskov, and R. K. Janev, Phys. Lett. A **84**, 243 (1981).
[15]V. A. Abramov, F. F. Baryshnikov, and V. S. Lisitsa [Zh. Eksp. Teor. Fiz. **74**, 897 (1978)] Sov. Phys. JETP **47**, 469 (1978).
[16]R. K. Janev, D. S. Belic, and B. H. Bransden, Phys. Rev. A **28**, 1293 (1983).
[17]B. H. Bransden, C. W. Newby, and C. J. Noble, J. Phys. B **13**, 4245 (1980).
[18]B. H. Bransden, C. W. Newby, and C. J. Noble, J. Phys. B **14**, L297 (1981).
[19]B. H. Bransden, C. W. Newby, and C. J. Noble, J. Phys. B **15**, 451 (1982).
[20]N. Fritsch, J. Phys. B **15**, L389 (1982).
[21]J. F. Reading, A. L. Ford, and R. L. Becker, J. Phys. B **14**, 1995 (1981).
[22]H. Ryufuku and T. Watanabe, Phys. Rev. A **18**, 2005 (1978).
[23]H. Ryufuku and T. Watanabe, Phys. Rev. A **19**, 1538 (1979).
[24]H. Ryufuku and T. Watanabe, Phys. Rev. A **20**, 1828 (1979).
[25]L. P. Presnyakov and A. D. Ulantsev [Kvant. Elektron. **1**, 2377 (1974)] Sov. J. Quant. Electron. **4**, 1320 (1975).
[26]R. E. Olson and A. Salop, Phys. Rev. A **16**, 531 (1977).
[27]T. P. Grozdanov, J. Phys. B **13**, 3835 (1980).
[28]F. T. Chan and J. Eichler, Phys. Rev. Lett. **42**, 58 (1979).
[29]F. T. Chan and J. Eichler, Phys. Rev. A **20**, 104 (1979).
[30]F. T. Chan and J. Eichler, Phys. Rev. A **20**, 1841 (1979).
[31]D. Belkic, R. Gayet, and A. Salin, Phys. Rep. **56**, 279 (1979).
[32]R. Shakeshaft, Phys. Rev. A **10**, 1096 (1974).
[33]H. S. W. Massey, E. H. S. Burhop, and H. B. Gilbody, *Electronic and Ionic Impact Phenomena*, 5 vols. (Oxford University, Oxford, 1969–1974).
[34]D. Basu, S. C. Mukherjee, and D. P. Sural, Phys. Rep. **42C**, 145 (1978).
[35]D. S. Belkic and R. K. Janev, J. Phys. B **6**, 1020 (1973).
[36]A. Msezane and D. F. Gallaher, J. Phys. B **6**, 2334 (1973).
[37]D. Rapp, J. Chem. Phys. **61**, 3777 (1974).
[38]D. Belkic and R. Gayet, J. Phys. B **10**, 1911 (1977).
[39]D. Belkic and R. McCarroll, J. Phys. B **10**, 1933 (1977).
[40]C. Bottcher, J. Phys. B **10**, L213 (1977).
[41]C. Harel and A. Salin, J. Phys. B **10**, 3511 (1977).
[42]R. E. Olson, A. Salop, R. A. Phaneuf, and F. W. Meyer, Phys. Rev. A **16**, 1867 (1977).
[43]A. Salop and R. E. Olson, Phys. Rev. A **16**, 1811 (1977).
[44]J. Vaaben and J. S. Briggs, J. Phys. B **10**, L521 (1977).
[45]E. L. Duman and B.M. Smirnov, Fiz. Plazmy **4**, 1161 (1978) [Sov. J. Plasma Phys. **4**, 650 (1978)].
[46]J. E. Golden, J. H. McGuire, and K. Omidvar, Phys. Rev. A **18**, 2373 (1978).
[47]J. Eichler and F. T. Chan, Phys. Rev. A **20**, 104 (1979).
[48]G. J. Hatton, N. F. Lane, and T. G. Winter, J. Phys. B **12**, L571 (1979).
[49]A. Salop, J. Phys. B **12**, 919 (1979).
[50]A. Salop and R. E. Olson, Phys. Rev. A **19**, 1921 (1979).
[51]A. Salop and R. E. Olson, Phys. Lett. A **71**, 407 (1979).
[52]D. S. F. Crothers and N. R. Todd, J. Phys. B **13**, 547 (1980).
[53]D. S. F. Crothers and N. R. Todd, J. Phys. B **13**, 2277 (1980).
[54]S. Datta and S. C. Mukherjee, J. Phys. B **13**, 539 (1980).
[55]H. P. Saha, N. Maiti, and N. C. Sil, J. Phys. B **13**, 327 (1980).
[56]B. H. Bransden and C. J. Noble, J. Phys. B **14**, 1849 (1981).
[57]J. I. Casaubon, R. D. Piacentini, and A. Salin, J. Phys. B **14**, L297 (1981).
[58]D. S. F. Crothers, J. Phys. B **14**, 1035 (1981).
[59]L. J. Dubé and J. S. Briggs, J. Phys. B **14**, 4595 (1981).
[60]J. K. M. Eichler, A. Tsuji, and T. Ishihara, Phys. Rev. A **23**, 2833 (1981).
[61]K. Fujiwara, J. Phys. B **14**, 3977 (1981).
[62]T. S. Ho, M. Lieber, and F. T. Chan, Phys. Rev. A **24**, 2925 (1981).
[63]M. Kimura and W. R. Thorson, Phys. Rev. A **24**, 3019 (1981).
[64]C. R. Mandal, S. Datta, and S. C. Mukherjee, Phys. Rev. A **24**, 3044 (1981).
[65]R. E. Olson, Phys. Rev. A **24**, 1726 (1981).
[66]L. P. Presnyakov, D. B. Uskov, and R. K. Janev, Ref. 14 and Zh. Eksp. Teor. Fiz. **83**, 933 (1982).
[67]B. H. Bransden and C. J. Noble, J. Phys. B **15**, 451 (1982).
[68]J. F. Reading, A. L. Ford, and R. L. Becker, J. Phys. B **15**, 625 (1982).
[69]H. Ryufuku, Phys. Rev. A **25**, 720 (1982).
[70]T. G. Winter, Phys. Rev. A **25**, 697 (1982).
[71]R. K. Janev, D. S. Belic, and R. H. Bransden, Ref. 16 and unpublished M-LZ-RC results.
[72]A. L. Ford, J. F. Reading, and R. L. Becker, J. Phys. B **15**, 3257 (1982).
[73]B. H. Bransden, J. Chandler, and C. J. Noble, 1982 (unpublished).
[74]B. H. Bransden, C. W. Newby, and C. J. Noble, 1982 (unpublished).
[75]E. J. Shipsey, T. A. Green, and J. C. Browne, Phys. Rev. A **27**, 821 (1983).
[76]J. E. Bayfield and G. A. Khayrallah, Phys. Rev. A **12**, 869 (1975).
[77]W. L. Nutt, R. W. McCullough, K. Brady, M. B. Shah, and H. B. Gilbody, J. Phys. B **11**, 1457 (1978).
[78]M. B. Shah and H. B. Gilbody, J. Phys. B **11**, 121 (1978).
[79]M. B. Shah, T. V. Goffe, and H. B. Gilbody, J. Phys. B **11**, L233 (1978).
[80]D. H. Crandall, R. A. Phaneuf, and F. W. Meyer, Phys. Rev. A **19**, 504 (1979).
[81]T. V. Goffe, M. B. Shah, and H. B. Gilbody, J. Phys. B **12**, 3763 (1979).
[82]F. W. Meyer, R. A. Phaneuf, H. J. Kim, P. Hvelplund, and P. H. Stelson, Phys. Rev. A **19**, 515 (1979).
[83]W. Seim, A. Müller, I. Wirkner-Bott, and E. Salzborn, J. Phys. B **14**, 3475 (1981).
[84]R. A. Phaneuf, I. Alvarez, F. W. Meyer, and D. H. Crandall, Phys. Rev. A **26**, 1892 (1982).